Received: 9 May 2022 | Revised: 5 May 2023 | Accepted: 16 August 2023

DOI: 10.1002/rnc.6966

RESEARCH ARTICLE

WILEY

Bearing-based formation control of second-order multiagent systems with bounded disturbances

Chuang Xu[1] | **Daniel Zelazo**[2] | **Baolin Wu**[3]

[1]Aerospace Time Feipeng Company Limited, Suzhou, People's Republic of China

[2]Faculty of Aerospace Engineering, Technion–Israel Institute of Technology, Haifa, Israel

[3]Research Center of Satellite Technology, Harbin Institute of Technology, Harbin, People's Republic of China

Correspondence
Baolin Wu, Research Center of Satellite Technology, Harbin Institute of Technology, Harbin, People's Republic of China.
Email: wuba0001@e.ntu.edu.sg

Funding information
National Natural Science Foundation of China, Grant/Award Number: 61873312

Abstract

This article investigates the bearing-based formation control problem for second-order multiagent systems (SMS) in the presence of the bounded disturbances in their models. The main contributions of this article are listed as follows: (1) We extend the bearing formation control to SMS. (2) We propose two novel robust distributed bearing formation control laws. In the first control law, the bearing measurement in the global inertial frame is required. This control law guarantees that the inter-agent bearings converge to the desired bearings. The second control law requires obtaining the local bearing measurements and relative orientation measurements. This control law guarantees that the inter-agent bearings converge to the desired bearings and the orientation of each agent converges to a common orientation. Some simulations are conducted, and simulation results verify the effectiveness of the proposed control laws.

KEYWORDS

attitude consensus, bearing measurement, formation control, second-order system

1 | INTRODUCTION

Formation control for multiagent systems has attracted much attention in recent years since it can be widely applied in many fields, such as robot formations,[1-4] unmanned aerial vehicles,[5,6] and spacecraft formation keeping.[7,8] Many approaches have been proposed for the formation control problem in the recent years. According to the measurements available to the systems, these approaches can be classified into three categories:[9,10] relative-position-based formation control approach (RPFCA),[1-8,11-14] distance-based formation control approach (DFCA),[10,15-17] and relative-bearing-based formation control approach (RBFCA).[18-24]

RPFCA and DFCA require measuring the relative position and distances between agents, respectively. However, it is not always easy to meet these requirements, especially for the agents that cannot access an external localization system.[25] Furthermore, in DFCA, the global stability cannot be guaranteed.[26-28] This is in part due to the presence of so-called flip ambiguities found in construction of rigid graphs, a tool commonly used in DFCA.[9,16,29,30] RBFCA requires measuring the relative bearings between agents. Compared with the relative position or distance measurements, the relative bearing measurements are often more accessible and cheaper,[31] and can be obtained by on-board camera[32] or sensor arrays.[33]

In RBFCA, the bearing rigidity theory (BRT) has proven to be an important tool.[18-24] Bearing rigidity provides a mathematically rigorous way to determine, for example, the uniqueness of a formation shape as parameterized by the set of bearing measurements available in a multiagent system. In References 18,19,21, the results on the BRT focused on the

[Correction added on 14 September 2023, after first online publication: affiliations 2 and 3 have been interchanged and the address in the Correspondence section has been updated.]

frameworks in 2-D space. In References 22 and 23, the BRT was extended to arbitrary dimensions. Based on the BRT,[34] proposed a prescribed-time bearing-only formation control law for single-integrator multiagent systems. It should be pointed out that most of the bearing-based results only focus on single-integrator, double-integrator or mobile robot systems.[18-24] The existing results often do not take disturbances in the dynamics into consideration. In fact, in many real-world applications, the agents in the formation are often characterized by dynamics with bounded disturbances. It is necessary, therefore, to study the bearing-based formation control problem for such systems. In Reference 9, an adaptive formation control law for multiple robot systems with a global frame was considered. However, the results in Reference 9 requires knowing the position of each agent and regression matrix of the system and cannot be applied straightforwardly to the system without a global frame.

In practice, it is not easy for a multiagent system to obtain a global frame. Compared with the methods that require to access a global frame, the methods without a global frame will have wider applications. In References 22 and 35, a rotation-matrix-based bearing rigidity approach and a quaternion-based bearing rigidity approach are respectively proposed for a single-integrator system without a global frame. However, the study on the bearing-based formation control for second-order system without a global frame is still an open issue.

This article investigates the problem of bearing-based formation control for second-order multiagent systems in the presence of bounded disturbances in their models. Two novel robust distributed bearing formation control laws are proposed for SMS with and without a global frame. In the control law with a global frame, a virtual velocity is firstly designed by using the relative bearing measurement in the global frame. When the velocities of agents track the virtual velocities, the inter-agent bearings can converge to the desired bearings. Then, a fixed-time velocity-tracking control law is proposed to track the virtual velocity. Under this control law, the inter-agent bearings converge to the desired bearings, and the virtual velocity converges to zero. In the control law without a global frame, a virtual velocity and a virtual angular velocity are designed by using the relative bearing measurement and relative orientation measurement in the local frame, respectively. Then, a fixed-time velocity-tracking control law and a fixed-time angular-velocity-tracking control law are proposed to track the virtual velocity and angular velocity, respectively. Under the control law without a global frame, the inter-agent bearings converge to the desired bearings, and the orientation of each agent converges to a common orientation. The system stability under the proposed two control laws are proven, and the simulation results also validate the effectiveness of the proposed control laws. The contributions of this article can be summarized as follows:

(i) We extend the bearing formation control to the SMS in the presence of the bounded disturbances. Different from the results in References 18,19,21-23,34, the proposed control schemes can deal with the problem of bearing-based formation control for SMS in the presence of the bounded disturbances.
(ii) Two novel distributed bearing formation control laws are proposed for SMS with and without a global frame, respectively. Compared with the methods in References 9,18-21,23,24 that require to access a global frame, the methods without a global frame will have wider applications.

This article is organized as follows. Some basic preliminaries from multiagent dynamical systems and bearing rigidity theory are provided in Section 2. The bearing formation control problems with and without a global inertial frame are given in Sections 3 and 4, respectively, and some simulation examples are provided in Section 5. Finally, the conclusion is discussed in Section 6.

Notations

The maximum and minimum eigenvalues of a matrix $\boldsymbol{A}$ are denoted by $\lambda_{\max}(\boldsymbol{A})$ and $\lambda_{\min}(\boldsymbol{A})$, respectively. The 2-norm of a matrix $\boldsymbol{A}$ is denoted $\|\boldsymbol{A}\|$. The vector $\mathbf{1}_n$ is defined as $\mathbf{1}_n = [1, \dots, 1]^T \in \mathbb{R}^{n\times 1}$. An identity matrix is denoted by $\boldsymbol{I}_n \in \mathbb{R}^{n\times n}$. The Kronecker product is denoted by $\otimes$. For two quaternions $\boldsymbol{Q} = [q_0;\ \boldsymbol{q}^T] \in \mathbb{R}^4$ and $\boldsymbol{P} = [p_0;\ \boldsymbol{p}^T] \in \mathbb{R}^4$, the quaternion composition is defined as $\boldsymbol{Q} \odot \boldsymbol{P} = [q_0p_0 - \boldsymbol{q}^T\boldsymbol{p};\ q_0\boldsymbol{p}^T + p_0\boldsymbol{q}^T + (\boldsymbol{q}\times\boldsymbol{p})^T] \in \mathbb{R}^4$. The matrix $\boldsymbol{P}(\boldsymbol{x}) = \boldsymbol{I}_n - \boldsymbol{x}\boldsymbol{x}^T/\|\boldsymbol{x}\|^2 \in \mathbb{R}^{n\times n}$ is the orthogonal projector operator of the nonzero vector $\boldsymbol{x} \in \mathbb{R}^n$. The null space and range space of a matrix $\boldsymbol{A}$ are denoted by $\mathrm{Null}(\boldsymbol{A})$ and $\mathrm{Range}(\boldsymbol{A})$, respectively. For a vector $\boldsymbol{x} = [x_1,\ x_2,\ \dots,\ x_n]^T \in \mathbb{R}^n$ and $\nu \in \mathbb{R}$, $\mathrm{sig}^{\nu}(\boldsymbol{x}) = [\mathrm{sign}(x_1)|x_1|^{\nu}, \dots, \mathrm{sign}(x_n)|x_n|^{\nu}]^T$, where $\mathrm{sign}(x_i)$ is the sign function.

A directed graph (digraph) $\mathcal{G} = (\mathcal{V}, \mathcal{E})$ contains a set of vertices $\mathcal{V} = \{1, \dots, n\}$ and a set of edges $\mathcal{E} \in \mathcal{V}\times\mathcal{V}$ with $m = |\mathcal{E}|$. The set $\mathcal{N}_i \triangleq \{j \in \mathcal{V} : (i,j) \in \mathcal{E}\}$ denotes the set of neighbors of the vertex i. A digraph is called *strongly connected* if every vertex is reachable from every other vertex by a directed path. Let $\overline{\boldsymbol{H}} = \boldsymbol{H} \otimes \boldsymbol{I}_3$. The incidence matrix $\boldsymbol{H} \in \mathbb{R}^{m\times n}$ is a $\{0, \pm 1\}$-matrix with $[\boldsymbol{H}]_{ki} = 1$ if the vertex i is the head of edge k, $[\boldsymbol{H}]_{ki} = -1$ if the vertex i is the tail of edge k, and $[\boldsymbol{H}]_{ki} = 0$ otherwise.

2 | PRELIMINARIES

We provide here some basic preliminaries from multiagent dynamical systems and BRT that will be needed for this work.

2.1 | Dynamics of multiagent systems

In this article, we consider multiagent systems containing n agents, where each agent has 6 degree of freedom and the state of an agent consists of its position and attitude. The motion dynamics of agent i is given as[36]

$$\begin{cases} \dot{\boldsymbol{x}}_i(t) = \boldsymbol{v}_i(t) \\ \dot{\boldsymbol{v}}_i(t) = \boldsymbol{f}_i(t) + \boldsymbol{\Delta}_{mi}(t) \end{cases}, \tag{1}$$

where $\boldsymbol{x}_i(t) \in \mathbb{R}^3$ is the position of agent i, $\boldsymbol{v}_i(t) \in \mathbb{R}^3$ is the velocity of agent i, $\boldsymbol{f}_i(t) \in \mathbb{R}^3$ is the control input, and $\boldsymbol{\Delta}_{mi}(t) \in \mathbb{R}^3$ is a bounded disturbance. The signals $\boldsymbol{x}_i(t)$, $\boldsymbol{v}_i(t)$, and $\boldsymbol{f}_i(t)$ are expressed in a global inertial frame.

The attitude dynamics and kinematics of agent i is modeled as[37]

$$\begin{cases} \dot{\boldsymbol{Q}}_i(t) = \frac{1}{2}\boldsymbol{M}(\boldsymbol{Q}_i(t))\boldsymbol{\omega}_i^+(t) \\ \boldsymbol{J}_i\dot{\boldsymbol{\omega}}_i(t) = -\boldsymbol{\omega}_i^\times(t)\boldsymbol{J}_i\boldsymbol{\omega}_i(t) + \boldsymbol{u}_i(t) + \boldsymbol{\Delta}_{ai}(t) \end{cases}, \tag{2}$$

where $\boldsymbol{J}_i \in \mathbb{R}^{3\times 3}$ denotes the inertia matrix of the agent i, $\boldsymbol{\omega}_i(t) \in \mathbb{R}^3$ represents the angular velocity of agent i expressed in the body-fixed frame $\mathcal{F}_{bi}$, $\boldsymbol{\omega}_i^+(t) = \left[0, \boldsymbol{\omega}_i^T(t)\right]^T \in \mathbb{R}^4$, $\boldsymbol{u}_i(t) \in \mathbb{R}^3$ denotes the control torque of agent i expressed in the body-fixed frame $\mathcal{F}_{bi}$, $\boldsymbol{\Delta}_{ai}(t) \in \mathbb{R}^3$ is the disturbance torques, the unit-quaternion $\boldsymbol{Q}_i(t) = \left[q_{0,i}(t), \boldsymbol{q}_i^T(t)\right]^T = \left[\cos\frac{\theta_i(t)}{2}, \boldsymbol{e}_i^T(t)\sin\frac{\theta_i(t)}{2}\right]^T \in \mathbb{R}^4$ represents the orientation of the body-fixed frame $\mathcal{F}_{bi}$ with respect to (w.r.t.) the global inertial frame $\mathcal{F}_I$, $\theta_i(t) \in \mathbb{R}$ and $\boldsymbol{e}_i(t) \in \mathbb{R}^3$ are the rotation angle and Euler axis of agent i, respectively, and the matrix $\boldsymbol{M}(\boldsymbol{Q}_i(t))$ is given by

$$\boldsymbol{M}(\boldsymbol{Q}_i(t)) = \begin{bmatrix} q_{0,i}(t) & -\boldsymbol{q}_i^T(t) \\ \boldsymbol{q}_i(t) & q_{0,i}(t)\boldsymbol{I}_3 + \boldsymbol{q}_i^\times(t) \end{bmatrix}. \tag{3}$$

For $\boldsymbol{x} = [x_1, x_2, x_3]^T$, $\boldsymbol{x}^\times \in \mathbb{R}^{3\times 3}$ is defined as

$$\boldsymbol{x}^\times = \begin{bmatrix} 0 & -x_3 & x_2 \\ x_3 & 0 & -x_1 \\ -x_2 & x_1 & 0 \end{bmatrix}. \tag{4}$$

For the sake of simplicity, the time (t) is omitted in the following parts of this article, that is, $\boldsymbol{x}_i(t) = \boldsymbol{x}_i, \boldsymbol{v}_i(t) = \boldsymbol{v}_i$, $\boldsymbol{f}_i(t) = \boldsymbol{f}_i, \boldsymbol{\Delta}_{mi}(t) = \boldsymbol{\Delta}_{mi}, \boldsymbol{Q}_i(t) = \boldsymbol{Q}_i, \boldsymbol{\omega}_i(t) = \boldsymbol{\omega}_i, \boldsymbol{u}_i(t) = \boldsymbol{u}_i$, and $\boldsymbol{\Delta}_{ai}(t) = \boldsymbol{\Delta}_{ai}$.

For two unit-quaternions $\boldsymbol{Q}_i$ and $\boldsymbol{Q}_j$, the error quaternion $\boldsymbol{Q}_{ij}$ is defined as[35]

$$\boldsymbol{Q}_{ij} = \boldsymbol{Q}_i^{-1} \odot \boldsymbol{Q}_j = \boldsymbol{M}\left(\boldsymbol{Q}_i^{-1}\right)\boldsymbol{Q}_j = \boldsymbol{N}\left(\boldsymbol{Q}_j\right)\boldsymbol{Q}_i^{-1}, \tag{5}$$

where $\boldsymbol{Q}_i^{-1} = \left[q_{0,i};\ -\boldsymbol{q}_i^T\right]$, and

$$\boldsymbol{N}\left(\boldsymbol{Q}_j\right) = \begin{bmatrix} q_{0,j} & -\boldsymbol{q}_j^T \\ \boldsymbol{q}_j & q_{0,j}\boldsymbol{I}_3 - \boldsymbol{q}_j^\times \end{bmatrix}. \tag{6}$$

2.2 | Bearing rigidity

A *framework* $\mathcal{G}(\boldsymbol{x})$ with $\boldsymbol{x} = [\boldsymbol{x}_1^T, \dots, \boldsymbol{x}_n^T]^T$ is an embedding of a graph into a metric space. The relative bearing of the agent i, w.r.t., the agent j expressed in the global inertial frame $\mathcal{F}_I$ is defined as

$$\boldsymbol{b}_{ij} = \frac{\boldsymbol{x}_j - \boldsymbol{x}_i}{\|\boldsymbol{x}_j - \boldsymbol{x}_i\|} = \frac{\boldsymbol{x}_{ij}}{\|\boldsymbol{x}_{ij}\|} \in \mathbb{R}^3. \tag{7}$$

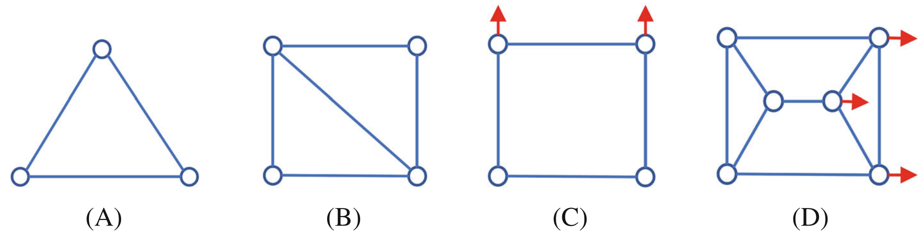

FIGURE 1 An illustration of infinitesimally bearing rigid. The frameworks in (A,B) are infinitesimally bearing rigid. The frameworks in (C,D) are not infinitesimally bearing rigid. The red/solid arrows denote nontrivial IBMs that can preserve all the inter-neighbor bearings.

A bearing function is defined to map the configuration $\boldsymbol{x}$ to bearings between agents connected by edges in the framework $\mathcal{G}(\boldsymbol{x})$,

$$\boldsymbol{b}_{\mathcal{G}}(\boldsymbol{x}) = \left[\boldsymbol{b}_1^T, \dots, \boldsymbol{b}_m^T\right]^T \in \mathbb{R}^{3m}, \tag{8}$$

where $\boldsymbol{b}_k$ $(k = 1, 2, \dots, m)$ is the bearing vector of the kth directed edge of $\mathcal{G}(\boldsymbol{x})$ and $m = |\mathcal{E}|$ is the number of edges in the framework $\mathcal{G}(\boldsymbol{x})$. Then, the *bearing rigidity matrix* $\boldsymbol{\Gamma}(\boldsymbol{x})$ is defined as[22]

$$\boldsymbol{\Gamma}(\boldsymbol{x}) \triangleq \frac{\partial \boldsymbol{b}_{\mathcal{G}}(\boldsymbol{x})}{\partial \boldsymbol{x}} = \operatorname{diag}\left(\frac{\boldsymbol{P}(\boldsymbol{b}_{ij})}{\|\boldsymbol{x}_{ij}\|}\right)_{(i,j)\in\mathcal{E}} (\boldsymbol{H} \otimes \boldsymbol{I}_3) \in \mathbb{R}^{3m\times 3n}. \tag{9}$$

Definition 1 (infinitesimal bearing motion (IBM)[22]). Define $\delta\boldsymbol{x}$ as a variation of the configuration $\boldsymbol{x}$. Then, a variation $\delta\boldsymbol{x}$ is called an infinitesimal bearing motion (IBM) of the framework $\mathcal{G}(\boldsymbol{x})$ if $\boldsymbol{\Gamma}(\boldsymbol{x})\delta\boldsymbol{x} = \boldsymbol{0}$. An IBM is called *trivial* if it corresponds to a translation and a scaling of the entire framework.

Definition 2 (infinitesimal bearing rigidity (IBR),[22] Definition 5). A framework $\mathcal{G}(\boldsymbol{x})$ is infinitesimally bearing rigid if all the IBMs are trivial.

To illustrate these definitions, some examples are given in Figure 1. The frameworks in Figure 1A,B are infinitesimally bearing rigid because all the IBMs are trivial. The frameworks in Figure 1C,D are not infinitesimally bearing rigid because there exist some nontrivial IBMs that can preserve all the inter-neighbor bearings.

2.3 | Definition of fixed-time stability and some lemmas

The definition of fixed-time stability and some lemmas are introduced to facilitate the stability analysis of the system in this section. Consider the following system

$$\dot{\boldsymbol{x}}(t) = \boldsymbol{f}(\boldsymbol{x}(t)),\ \boldsymbol{x}(t) \in \mathbb{R}^d, \tag{10}$$

where $\boldsymbol{f}(\boldsymbol{x}(t)) :\ \mathbb{R}^d \to \mathbb{R}^d$ is a continuous function with $\boldsymbol{f}(\boldsymbol{0}) = \boldsymbol{0}$.

Definition 3. The origin of system (10) is called fixed-time stable if it is globally asymptotically stable and any solution $\boldsymbol{x}(t)$ of (10) reaches the origin in a fixed time, that is, $\lim_{t\to T} \boldsymbol{x}(t) = \boldsymbol{0}$, $\forall \boldsymbol{x}(0) \in \mathbb{R}^d$, where the settling time T is a positive constant.

Lemma 1 (38, Lemma 1). *If there is a continuous function $V(\boldsymbol{x}(t)) : \mathbb{R}^d \to \mathbb{R}_+ \cup \{0\}$ satisfying (i) $V(\boldsymbol{x}(t)) = 0 \Leftrightarrow \boldsymbol{x} = \boldsymbol{0}$ and (ii) $\frac{\mathrm{d}V(\boldsymbol{x}(t))}{\mathrm{d}t} \le -\left(\alpha V(\boldsymbol{x}(t))^p + \beta V(\boldsymbol{x}(t))^q\right)^v$, where $\alpha,\ \beta,\ p,\ q$ and v are positive constants, $pv < 1$, $qv > 1$, then the origin of the system (10) is globally fixed-time stable with a settling time*

$$T \le \frac{1}{\alpha^v(1 - pv)} + \frac{1}{\beta^v(qv - 1)}. \tag{11}$$

Lemma 2 (39, Lemmas 3.3 and 3.4). *Let $x_1, x_2, \dots, x_n \ge 0$. If $0 < v \le 1$,*

$$\sum_{i=1}^{n} x_i^v \ge \left(\sum_{i=1}^{n} x_i\right)^v. \tag{12}$$

If $v > 1$,

$$\sum_{i=1}^{n} x_i^v \geq n^{1-v}\left(\sum_{i=1}^{n} x_i\right)^v. \tag{13}$$

3 | BEARING FORMATION CONTROL WITH A GLOBAL INERTIAL FRAME

This section studies the formation control problem where a global inertial frame is available to each agent, and each agent can measure their own velocities and relative bearings w.r.t. their neighboring agents in a global inertial frame.

3.1 | Bearing formation control law and stability analysis

Denote $\{\boldsymbol{b}_{ij}^\star\}_{(i,j)\in\mathcal{E}}$ as the set of desired bearings between the agents. The following assumptions are now required.

Assumption 1. There exists a feasible configuration $\boldsymbol{x}^\star$ that satisfies the fixed desired bearings $\{\boldsymbol{b}_{ij}^\star\}_{(i,j)\in\mathcal{E}}$, and the framework $\mathcal{G}(\boldsymbol{x}^\star)$ is infinitesimal bearing rigid.

According to Theorem 6 in References 22, any IBR frameworks are unique. Thus, Assumption 1 guarantees that the desired framework $\mathcal{G}(\boldsymbol{x}^\star)$ is unique. If the desired framework $\mathcal{G}(\boldsymbol{x}^\star)$ is not unique, no control approaches can guarantee to achieve the desired framework $\mathcal{G}(\boldsymbol{x}^\star)$.[24]

Assumption 2. No agent collides with its neighbors, that is, $\|\boldsymbol{x}_{ij}\| \geq d_{\min}, \forall i,j \in \mathcal{N}$ with $d_{\min} > 0$ being a constant.

Assumption 3. The disturbance $\boldsymbol{\Delta}_{mi}$ and disturbance torque $\boldsymbol{\Delta}_{ai}$ of each agent are bounded by known upper bounds ϵ_1 and ϵ_2, respectively, that is, $\|\boldsymbol{\Delta}_{mi}\| \leq \epsilon_1$ and $\|\boldsymbol{\Delta}_{ai}\| \leq \epsilon_2$.

The control problem we aim to solve in this section is stated as follows:

Problem 1. Design control inputs $\boldsymbol{f}_i$ for the agents described by (1) using the inter-agent bearing measurements $\boldsymbol{b}_{ij}$ such that the inter-agent bearing $\boldsymbol{b}_{ij}$ converges to the desired bearing $\boldsymbol{b}_{ij}^\star$, that is, $\lim_{t\to\infty} \boldsymbol{b}_{ij} = \boldsymbol{b}_{ij}^\star$, $\forall (i,j) \in \mathcal{E}$.

The formation control law is designed as

$$\begin{cases} \boldsymbol{f}_i = -\alpha_1 \boldsymbol{s}_{vi} - \alpha_2 \mathrm{sig}^{r_1}(\boldsymbol{s}_{vi}) - \alpha_3 \mathrm{sig}^{r_2}(\boldsymbol{s}_{vi}) - \alpha_4 \mathrm{sign}(\boldsymbol{s}_{vi}) \\ \boldsymbol{v}_{vi} = -\alpha_5 \sum\limits_{j\in\mathcal{N}_i} \boldsymbol{P}(\boldsymbol{b}_{ij})\boldsymbol{b}_{ij}^\star \end{cases}, \tag{14}$$

where $\boldsymbol{s}_{vi} = \boldsymbol{v}_i - \boldsymbol{v}_{vi}$, $\boldsymbol{v}_{vi} \in \mathbb{R}^3$ is a virtual velocity, $\alpha_k (k = 1,2,3,4,5)$, $r_1 < 1$ and $r_2 > 1$ are some positive constants, and $\boldsymbol{b}_{ij}^\star$ is the desired bearing of the agent i, w.r.t., the agent j expressed in the global inertial frame.

As is shown in Figure 2, the formation control is divided into two steps in this section. In the first step, the velocity $\boldsymbol{v}_i$ converges to the designed virtual velocity $\boldsymbol{v}_{vi}$ in a fixed time under the control law (14). In the second step, the inter-agent bearings converge to the desired bearings when the velocities $\boldsymbol{v}_i$ track the virtual velocities $\boldsymbol{v}_{vi}$. Thus, the stability analysis of the system is also divided into two steps. The first step proves that the velocity $\boldsymbol{v}_i$ converges to the designed virtual velocity $\boldsymbol{v}_{vi}$ in a fixed time under the control law (14). The second step proves that the inter-agent bearings converge to the desired bearings when the velocities $\boldsymbol{v}_i$ track the virtual velocities $\boldsymbol{v}_{vi}$.

Note that the controller (14) is discontinuous at $\boldsymbol{s}_{vi} = \boldsymbol{0}$. To address this problem, a Filippov solution is introduced.

Definition 4 (Filippov solution[40]). An absolutely continuous function $\boldsymbol{\phi}(t)$ defined on the interval $[0,\ T]$ is called a Filippov solution of $\dot{\boldsymbol{x}} = \mathbf{g}(\boldsymbol{x})$ if for almost all $t \in [0,\ T]$,

$$\dot{\boldsymbol{\phi}}(t) \in \mathcal{K}(\mathbf{g}(\boldsymbol{x})) \triangleq \bigcap_{\varepsilon>0} \bigcap_{\mu(N)=0} \mathrm{co}\{\mathbf{g}(\boldsymbol{B}(\boldsymbol{x},\varepsilon) - N)\},\ \boldsymbol{\phi}(0) = \boldsymbol{x}_0, \tag{15}$$

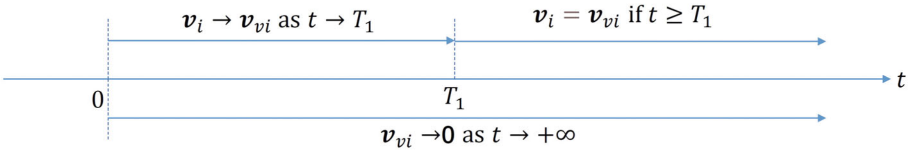

FIGURE 2 The control process under the formation control law (14).

where $\boldsymbol{B}(\boldsymbol{x}, \varepsilon) = \{\boldsymbol{y} : \|\boldsymbol{y} - \boldsymbol{x}\| \leq \varepsilon\}$, $\mathrm{co}\{\cdot\}$ denotes the convex closure, μ is n dimensional Lebesgue measure, and N is an arbitrary set in $\mathbb{R}^n$.

Theorem 1. *Consider a multiagent system described by (1). If Assumptions 1-3 hold,* $\alpha_4 \geq \max_{i=1,\dots,n}\{|\mathcal{N}_i|\}\frac{4\alpha_5 V_{M1}}{d_{\min}} + \epsilon_1$, *and the initial velocities satisfy* $\|\boldsymbol{v}_i(0)\| \leq V_{M1}$ *with* $V_{M1} > 0$ *being a large constant, the errors* $\boldsymbol{s}_{vi}$ *converges to the origin in a fixed time with a settling time* T_1 *under the control law in (14), where* T_1 *is defined as*

$$T_1 = \frac{2}{\eta_1(1 - r_1)} + \frac{2}{\eta_2(r_2 - 1)}, \tag{16}$$

with $\eta_1 = \alpha_2 2^{\frac{1+r_1}{2}}$ *and* $\eta_2 = \alpha_3 2^{\frac{1+r_2}{2}} n^{\frac{1-r_2}{2}}$.

Proof. See Appendix A. ∎

Remark 1. In Theorem 1, it is required that the control parameter α_4 should satisfy the inequality $\alpha_4 \geq \max_{i=1,\dots,n}\{|\mathcal{N}_i|\}\frac{4\alpha_5 V_{M1}}{d_{\min}} + \epsilon_1$. If the disturbance Δ_i is very large or even unbounded, it is difficult to guarantee this inequality holds, since the parameter α_4 should not be very large to avoid violent chattering of the control input. Therefore, it is necessary to assume that the disturbance Δ_i is bounded by a constant ϵ_1.

In Theorem 1, we have proven that $\boldsymbol{v}_i = \boldsymbol{v}_{vi}$ after the time T_1 under the control law (14). Then, the motion dynamics in (1) becomes $\dot{\boldsymbol{x}}_i = \boldsymbol{v}_{vi}$ after the time T_1 under the control law (14). Next, we need to prove that $\lim_{t\to\infty} \boldsymbol{b}_{ij}(t) = \boldsymbol{b}_{ij}^{\star}, \forall (i,j) \in \mathcal{E}$ under the control law (14). The basic idea of the proof is to prove that the formation $\mathcal{G}(\boldsymbol{x})$ converges to a desired formation $\mathcal{G}(\boldsymbol{x}^{\star})$ defined in Definition 5.

Definition 5 (desired formation). Denote $\mathcal{G}(\boldsymbol{x}^{\star})$ as a desired formation such that it has the same bearings with the desired bearings $\{\boldsymbol{b}_{ij}^{\star}\}_{(i,j)\in\mathcal{E}}$, that is, $\left(\boldsymbol{x}_j^{\star} - \boldsymbol{x}_i^{\star}\right)/\|\boldsymbol{x}_j^{\star} - \boldsymbol{x}_i^{\star}\| = \boldsymbol{b}_{ij}^{\star}, \forall (i,j) \in \mathcal{E}$.

The scale l and centroid $\bar{\boldsymbol{x}}$ of the formation are defined as

$$l = \sqrt{\frac{1}{n}\sum_{i=1}^{n}\|\boldsymbol{x}_i - \bar{\boldsymbol{x}}\|^2}, \quad \text{and} \quad \bar{\boldsymbol{x}} = \frac{1}{n}\sum_{i=1}^{n}\boldsymbol{x}_i. \tag{17}$$

Theorem 2. *Given the multiagent systems described by (1), the errors* $\boldsymbol{x}_e = \boldsymbol{x} - \boldsymbol{x}^{\star}$ *converge asymptotically to* $\boldsymbol{x}_e = \boldsymbol{0}$ *under the control law (14).*

Proof. Choose the Lyapunov function as

$$V_{x_e} = \frac{1}{2}\|\boldsymbol{x}_e\|^2. \tag{18}$$

The time derivative of V_{x_e} is

$$\begin{aligned} \dot{V}_{x_e} &= \left(\boldsymbol{x} - \boldsymbol{x}^{\star}\right)^T \dot{\boldsymbol{x}} \\ &= \left(\boldsymbol{x} - \boldsymbol{x}^{\star}\right)^T (\boldsymbol{v}_v + \boldsymbol{s}_v) \\ &= -\left(\boldsymbol{x}^{\star}\right)^T \boldsymbol{v}_v + \boldsymbol{x}_e^T \boldsymbol{s}_v, \end{aligned} \tag{19}$$

where $\boldsymbol{v}_v = \left[\boldsymbol{v}_{v1}^T, \dots, \boldsymbol{v}_{vn}^T\right]^T$, $\boldsymbol{s}_v = \left[\boldsymbol{s}_{v1}^T, \dots, \boldsymbol{s}_{vn}^T\right]^T$, and the property $\boldsymbol{v}_v \perp \mathrm{span}\{\boldsymbol{x}\}$ Reference 22(Lemma 5) is applied.

The proof is divided into two phases: $t \in [0, T_1)$ and $t \in [T_1, \infty)$, where T_1 is defined in (16). In the phase $t \in [0, T_1)$, we prove that $\boldsymbol{x}_e$ is bounded. In the phase $t \in [T_1, \infty)$, we prove that the errors $\boldsymbol{x}_e$ converge asymptotically to the origin.

Phase $t \in [0, T_1)$: Substituting $\boldsymbol{\nu}_{vi}$ in (14) into $\dot{V}_{x_e}$ yields

$$\begin{aligned}
\dot{V}_{x_e} &= -\alpha_5 \left(\boldsymbol{x}^\star\right)^T \overline{\boldsymbol{H}}^T \mathrm{diag}(\boldsymbol{P}(\boldsymbol{b}_k))\boldsymbol{b}^\star + \boldsymbol{x}_e^T \boldsymbol{s}_v \\
&= -\alpha_5 \left(\boldsymbol{e}^\star\right)^T \mathrm{diag}(\boldsymbol{P}(\boldsymbol{b}_k))\boldsymbol{b}^\star + \boldsymbol{x}_e^T \boldsymbol{s}_v \\
&= -\alpha_5 \sum_{k=1}^{m} \left(\boldsymbol{e}_k^\star\right)^T \boldsymbol{P}(\boldsymbol{b}_k)\boldsymbol{b}_k^\star + \boldsymbol{x}_e^T \boldsymbol{s}_v \\
&= -\alpha_5 \sum_{k=1}^{m} \|\boldsymbol{e}_k^\star\| \left(\boldsymbol{b}_k^\star\right)^T \boldsymbol{P}(\boldsymbol{b}_k)\boldsymbol{b}_k^\star + \boldsymbol{x}_e^T \boldsymbol{s}_v,
\end{aligned} \tag{20}$$

where $\overline{\boldsymbol{H}} = \boldsymbol{H} \otimes \boldsymbol{I}_3$, $\boldsymbol{b}^\star = \left[\left(\boldsymbol{b}_1^\star\right)^T, \dots, \left(\boldsymbol{b}_m^\star\right)^T\right]^T$, $\boldsymbol{e}^\star = \left[\left(\boldsymbol{e}_1^\star\right)^T, \dots, \left(\boldsymbol{e}_m^\star\right)^T\right]^T$, $\boldsymbol{e}_k^\star = \boldsymbol{x}_j^\star - \boldsymbol{x}_i^\star$, $\forall k \in \{1, \dots, m\}$, $\boldsymbol{e}^\star = \overline{\boldsymbol{H}}\boldsymbol{x}^\star$.

According to Theorem 1, it follows that $\|\boldsymbol{s}_v(t)\| \le \|\boldsymbol{s}_v(0)\|$. Then,

$$\|\boldsymbol{\nu}_i\| = \|\boldsymbol{s}_{vi} + \boldsymbol{\nu}_{vi}\| \le \|\boldsymbol{s}_{vi}\| + \|\boldsymbol{\nu}_{vi}\| \le \|\boldsymbol{s}_{vi}(0)\| + n\alpha_5, \tag{21}$$

$$\begin{aligned}
\|\boldsymbol{x}_i(t)\| &= \left\|\boldsymbol{x}_i(0) + \int_0^t \boldsymbol{\nu}_i \mathrm{d}z\right\| \le \|\boldsymbol{x}_i(0)\| + \int_0^{T_1} \|\boldsymbol{\nu}_i\| dz \\
&\le \|\boldsymbol{x}_i(0)\| + T_1(\|\boldsymbol{s}_{vi}(0)\| + n\alpha_5),
\end{aligned} \tag{22}$$

$$\|\boldsymbol{e}_k\| = \|\boldsymbol{x}_i - \boldsymbol{x}_j\| \le \|\boldsymbol{x}_i\| + \|\boldsymbol{x}_j\| \le \sqrt{2}\|\boldsymbol{x}(0)\| + \sqrt{2}T_1\|\boldsymbol{s}_v(0)\| + 2T_1 n\alpha_5. \tag{23}$$

According to References 22(Lemma 8), it follows that $\left(\boldsymbol{b}_k^\star\right)^T \boldsymbol{P}(\boldsymbol{b}_k)\boldsymbol{b}_k^\star = \boldsymbol{b}_k^T \boldsymbol{P}\left(\boldsymbol{b}_k^\star\right)\boldsymbol{b}_k$. Then, (20) becomes

$$\begin{aligned}
\dot{V}_{x_e} &= -\alpha_5 \sum_{k=1}^{m} \|\boldsymbol{e}_k^\star\| \boldsymbol{b}_k^T \boldsymbol{P}\left(\boldsymbol{b}_k^\star\right)\boldsymbol{b}_k + \boldsymbol{x}_e^T \boldsymbol{s}_v = -\alpha_5 \sum_{k=1}^{m} \frac{\|\boldsymbol{e}_k^\star\|}{\|\boldsymbol{e}_k\|^2} \boldsymbol{e}_k^T \boldsymbol{P}\left(\boldsymbol{b}_k^\star\right)\boldsymbol{e}_k + \boldsymbol{x}_e^T \boldsymbol{s}_v \\
&\le -\underbrace{\frac{\alpha_5 \min_{k=1,\dots,m} \|\boldsymbol{e}_k^\star\|}{(\sqrt{2}\|\boldsymbol{x}(0)\| + \sqrt{2}T_1\|\boldsymbol{s}_v(0)\| + 2T_1 n\alpha_5)^2}}_{\mu_1} \sum_{k=1}^{m} \boldsymbol{e}_k^T \boldsymbol{P}\left(\boldsymbol{b}_k^\star\right)\boldsymbol{e}_k + \boldsymbol{x}_e^T \boldsymbol{s}_v \\
&= -\mu_1 \boldsymbol{e}^T \mathrm{diag}\left(\boldsymbol{P}\left(\boldsymbol{b}_k^\star\right)\right)\boldsymbol{e} + \boldsymbol{x}_e^T \boldsymbol{s}_v = -\mu_1 \boldsymbol{x}^T \overline{\boldsymbol{H}}^T \mathrm{diag}\left(\boldsymbol{P}\left(\boldsymbol{b}_k^\star\right)\right)\overline{\boldsymbol{H}}\boldsymbol{x} + \boldsymbol{x}_e^T \boldsymbol{s}_v \\
&= -\mu_1 \boldsymbol{x}_e^T \overline{\boldsymbol{H}}^T \mathrm{diag}\left(\boldsymbol{P}\left(\boldsymbol{b}_k^\star\right)\right)\overline{\boldsymbol{H}}\boldsymbol{x}_e + \boldsymbol{x}_e^T \boldsymbol{s}_v \text{ (due to } \mathrm{diag}\left(\boldsymbol{P}\left(\boldsymbol{b}_k^\star\right)\right)\overline{\boldsymbol{H}}\boldsymbol{x}^\star = 0) \\
&= -\mu_1 \boldsymbol{x}_e^T \underbrace{\overline{\boldsymbol{H}}^T \mathrm{diag}\left(\boldsymbol{P}\left(\boldsymbol{b}_k^\star\right)\right)}_{\overline{\boldsymbol{\Gamma}}^T(\boldsymbol{x}^\star)} \underbrace{\mathrm{diag}\left(\boldsymbol{P}\left(\boldsymbol{b}_k^\star\right)\right)\overline{\boldsymbol{H}}}_{\overline{\boldsymbol{\Gamma}}(\boldsymbol{x}^\star)}\boldsymbol{x}_e + \boldsymbol{x}_e^T \boldsymbol{s}_v,
\end{aligned} \tag{24}$$

where $\boldsymbol{e} = \left[\boldsymbol{e}_1^T, \dots, \boldsymbol{e}_m^T\right]^T$, $\boldsymbol{e}_k = \boldsymbol{x}_j - \boldsymbol{x}_i$, $\boldsymbol{e} = \overline{\boldsymbol{H}}\boldsymbol{x}$. The matrix $\overline{\boldsymbol{\Gamma}}\left(\boldsymbol{x}^\star\right)$ has the same null space and rank with the bearing rigidity matrix $\boldsymbol{\Gamma}\left(\boldsymbol{x}^\star\right)$ defined in (9). According to References 22(Theorem 4), it follows that $\mathrm{Null}\left(\boldsymbol{\Gamma}\left(\boldsymbol{x}^\star\right)\right) = \mathrm{span}\left(\boldsymbol{1} \otimes \boldsymbol{I}_3, \boldsymbol{x}^\star\right)$ and $\mathrm{rank}\left(\boldsymbol{\Gamma}\left(\boldsymbol{x}^\star\right)\right) = 3n - 4$ under Assumption 1. Thus, the smallest 4 eigenvalues of the matrix $\overline{\boldsymbol{\Gamma}}^T\left(\boldsymbol{x}^\star\right)\overline{\boldsymbol{\Gamma}}\left(\boldsymbol{x}^\star\right)$ are 0. Then, it follows from (24) that

$$\begin{aligned}
\dot{V}_{x_e} &\le -2\mu_1\lambda_5 V_{x_e} + \boldsymbol{x}_e^T \boldsymbol{s}_v \\
&\le -2\mu_1\lambda_5 V_{x_e} + \frac{\mu_1\lambda_5}{2}\|\boldsymbol{x}_e\|^2 + \frac{1}{2\mu_1\lambda_5}\|\boldsymbol{s}_v\|^2 \\
&= -\mu_1\lambda_5 V_{x_e} + \frac{1}{2\mu_1\lambda_5}\|\boldsymbol{s}_v\|^2,
\end{aligned} \tag{25}$$

where λ_5 is the minimum positive eigenvalue of $\overline{\boldsymbol{\Gamma}}^T(\boldsymbol{x}^\star)\overline{\boldsymbol{\Gamma}}(\boldsymbol{x}^\star)$. It follows from Theorem 1 that $\|\boldsymbol{s}_v(t)\| \le \|\boldsymbol{s}_v(0)\|$. Then, (25) yields

$$\dot{V}_{x_e} \le -\mu_1\lambda_5 V_{x_e} + \frac{1}{2\mu_1\lambda_5}\|\boldsymbol{s}_v(0)\|^2. \tag{26}$$

If $V_{x_e} > \frac{1}{2(\mu_1\lambda_5)^2}\|\boldsymbol{s}_v(0)\|^2$, that is, $\|\boldsymbol{x}_e\| > \frac{1}{\mu_1\lambda_5}\|\boldsymbol{s}_v(0)\| \triangleq \delta_{x_e}$, it follows from (26) that $\dot{V}_{x_e} < 0$ holds and $\boldsymbol{x}_e$ converges to the region $\left\{\boldsymbol{x}_e \middle| \|\boldsymbol{x}_e\| \le \delta_{x_e}\right\}$. If $V_{x_e} \le \frac{1}{2(\mu_1\lambda_5)^2}\|\boldsymbol{s}_v(0)\|^2$, it is obvious that $\boldsymbol{x}_e$ stays in the region $\left\{\boldsymbol{x}_e \middle| \|\boldsymbol{x}_e\| \le \delta_{x_e}\right\}$. Thus, $\boldsymbol{x}_e$ is bounded during $t \in [0, T_1)$.

Phase $t \in [T_1, \infty)$: According to Theorem 1, $\boldsymbol{s}_{vi} = 0$ after the time T_1. Then, following the similar proof of the phase $t \in [0, T_1)$, it follows

$$\dot{V}_{x_e} \le -2\mu_1\lambda_5 V_{x_e}. \tag{27}$$

Therefore, the errors $\boldsymbol{x}_e$ converge asymptotically to the origin when $t \in [T_1, \infty)$. ∎

3.2 | Collision avoidance

Theorem 1 is dependent on the assumption that no agent collides with its neighbors (Assumption 2). If two agents collide, the stability result may be invalid. However, the control law (14) cannot guarantee that no agent collides with its neighbors along trajectories. In this section, a sufficient condition is provided to guarantee that each agent maintains a minimum distance with its neighbors. That is, agents satisfying these conditions will satisfy Assumption 2 along the system trajectories.

Theorem 3. *Under Assumption 1 and the formation control law (14), if the initial states $\boldsymbol{x}_e(0)$ and $\boldsymbol{s}_v(0)$ satisfy*

$$\|\boldsymbol{x}_e(0)\| < \frac{1}{\sqrt{n}}\left(\min_{i,j\in\mathcal{V}}\|\boldsymbol{x}_i^\star - \boldsymbol{x}_j^\star\| - d_{\min}\right), \tag{28}$$

and

$$\|\boldsymbol{s}_v(0)\| < \frac{\mu_1\lambda_5}{\sqrt{n}}\left(\min_{i,j\in\mathcal{V}}\|\boldsymbol{x}_i^\star - \boldsymbol{x}_j^\star\| - d_{\min}\right), \tag{29}$$

where μ_1 is defined in (24), λ_5 is the minimum positive eigenvalue of $\overline{\boldsymbol{\Gamma}}^T(\boldsymbol{x}^\star)\overline{\boldsymbol{\Gamma}}(\boldsymbol{x}^\star)$, $\overline{\boldsymbol{\Gamma}}(\boldsymbol{x}^\star)$, and T_1 are defined in (24) and (16), respectively, then it can be guaranteed that

$$\|\boldsymbol{x}_i(t) - \boldsymbol{x}_j(t)\| > d_{\min} > 0,\ \forall i,j \in \mathcal{V},\ \forall t \ge 0.$$

Proof. For any $i,j \in \mathcal{V}$ and $t \ge 0$, we have

$$\begin{aligned}
\|\boldsymbol{x}_i(t) - \boldsymbol{x}_j(t)\| &= \|[\boldsymbol{x}_i(t) - \boldsymbol{x}_i^\star] - [\boldsymbol{x}_j(t) - \boldsymbol{x}_j^\star] + [\boldsymbol{x}_i^\star - \boldsymbol{x}_j^\star]\| \\
&\ge \|\boldsymbol{x}_i^\star - \boldsymbol{x}_j^\star\| - \|\boldsymbol{x}_i(t) - \boldsymbol{x}_i^\star\| - \|\boldsymbol{x}_j(t) - \boldsymbol{x}_j^\star\| \\
&\ge \|\boldsymbol{x}_i^\star - \boldsymbol{x}_j^\star\| - \sum_{i=1}^{n}\|\boldsymbol{x}_i(t) - \boldsymbol{x}_i^\star\| \\
&\ge \|\boldsymbol{x}_i^\star - \boldsymbol{x}_j^\star\| - \sqrt{n}\|\boldsymbol{x}(t) - \boldsymbol{x}^\star\| \\
&= \|\boldsymbol{x}_i^\star - \boldsymbol{x}_j^\star\| - \sqrt{n}\|\boldsymbol{x}_e(t)\|.
\end{aligned} \tag{30}$$

Denote $\delta_{x_e} = \frac{1}{\mu_1\lambda_5}\|\boldsymbol{s}_v(0)\|$. The proof is divided into two cases: $\|\boldsymbol{x}_e\| > \delta_{x_e}$ and $\|\boldsymbol{x}_e\| \le \delta_{x_e}$. If $\|\boldsymbol{x}_e(0)\| > \delta_{x_e}$, it follows from the proof of Theorem 2 that $\|\boldsymbol{x}_e(0)\| \ge \|\boldsymbol{x}_e(t)\|$. Then, (30) yields

$$\|\boldsymbol{x}_i(t) - \boldsymbol{x}_j(t)\| \ge \|\boldsymbol{x}_i^\star - \boldsymbol{x}_j^\star\| - \sqrt{n}\|\boldsymbol{x}_e(0)\| > d_{\min}. \tag{31}$$

Then, we have

$$\delta_{x_e} < \|\boldsymbol{x}_e(0)\| < \frac{1}{\sqrt{n}}\left(\min_{i,j\in\mathcal{V}} \|\boldsymbol{x}_i^\star - \boldsymbol{x}_j^\star\| - d_{\min}\right). \tag{32}$$

If $\|\boldsymbol{x}_e(0)\| \leq \delta_{x_e}$, it follows from the proof of Theorem 2 that $\|\boldsymbol{x}_e(t)\| \leq \delta_{x_e}$. Then, (30) yields

$$\|\boldsymbol{x}_i(t) - \boldsymbol{x}_j(t)\| \geq \|\boldsymbol{x}_i^\star - \boldsymbol{x}_j^\star\| - \sqrt{n}\delta_{x_e} > d_{\min}. \tag{33}$$

Then, we have

$$\|\boldsymbol{x}_e(0)\| \leq \delta_{x_e} < \frac{1}{\sqrt{n}}\left(\min_{i,j\in\mathcal{V}} \|\boldsymbol{x}_i^\star - \boldsymbol{x}_j^\star\| - d_{\min}\right). \tag{34}$$

Therefore, it can be obtained from the above analysis that if

$$\|\boldsymbol{x}_e(0)\| < \frac{1}{\sqrt{n}}\left(\min_{i,j\in\mathcal{V}} \|\boldsymbol{x}_i^\star - \boldsymbol{x}_j^\star\| - d_{\min}\right), \tag{35}$$

and

$$\|\boldsymbol{s}_v(0)\| < \frac{\mu_1\lambda_5}{\sqrt{n}}\left(\min_{i,j\in\mathcal{V}} \|\boldsymbol{x}_i^\star - \boldsymbol{x}_j^\star\| - d_{\min}\right). \tag{36}$$

■

The formation control law (14) solves the formation control problem where a global inertial frame is available to each agent. However, it is not easy for a multiagent system to obtain a global frame. Thus, it is necessary to study the formation control problem without a global inertial frame.

4 | BEARING FORMATION CONTROL WITHOUT A GLOBAL INERTIAL FRAME

This section studies the formation control problem where the agents cannot access the global inertial frame, that is, the relative bearings and orientations can be measured only in the body-fixed frames of the agents.

4.1 | Bearing formation control law

Denote $\boldsymbol{v}_i^b = \boldsymbol{R}(\boldsymbol{Q}_i)\boldsymbol{v}_i$, $\boldsymbol{f}_i^b = \boldsymbol{R}(\boldsymbol{Q}_i)\boldsymbol{f}_i$, and $\boldsymbol{\Delta}_{mi}^b = \boldsymbol{R}(\boldsymbol{Q}_i)\boldsymbol{\Delta}_{mi}$ as the velocity, control input and the disturbance of the agent i expressed in the body-fixed frame $\mathcal{F}_{bi}$, where $\boldsymbol{R}(\boldsymbol{Q}_i) = \left(q_{0,i}^2 - \boldsymbol{q}_i^T\boldsymbol{q}_i\right)\boldsymbol{I}_3 + 2\boldsymbol{q}_i\boldsymbol{q}_i^T - 2q_{0,i}\boldsymbol{q}_i^\times \in \mathbb{R}^{3\times 3}$ is the rotation matrix from the global inertial frame to the body-fixed frame $\mathcal{F}_{bi}$. Then, the dynamics in (1) can be rewritten as

$$\begin{cases} \dot{\boldsymbol{x}}_i = \boldsymbol{R}^T(\boldsymbol{Q}_i)\boldsymbol{v}_i^b \\ \dot{\boldsymbol{v}}_i^b = \boldsymbol{f}_i^b + \boldsymbol{\Delta}_{mi}^b + \boldsymbol{R}(\boldsymbol{Q}_i)\boldsymbol{\omega}_i^\times\boldsymbol{R}^T(\boldsymbol{Q}_i)\boldsymbol{v}_i^b \end{cases}. \tag{37}$$

The relative bearing $\boldsymbol{b}_{ij}^b$ expressed in the body-fixed frame $\mathcal{F}_{bi}$ is defined as

$$\boldsymbol{b}_{ij}^b = \boldsymbol{R}(\boldsymbol{Q}_i)\boldsymbol{b}_{ij}. \tag{38}$$

In this section, the control problem is stated as follows:

Problem 2. Design control inputs $\boldsymbol{f}_i^b$ and $\boldsymbol{u}_i$ for the agents described by (2) and (37) using the inter-agent bearing measurements $\boldsymbol{b}_{ij}^b$ and the inter-agent orientation measurements $\boldsymbol{Q}_{ij}$ such that

(i) the inter-agent bearings $\boldsymbol{b}_{ij}^b$ converge to the desired bearing $\boldsymbol{b}_{ij}^{b\star}$, that is, $\lim_{t\to\infty} \boldsymbol{b}_{ij}^b = \boldsymbol{b}_{ij}^{b\star}$, $\forall(i,j) \in \mathcal{E}$.
(ii) the orientation of each agent converges to a common orientation, that is, $\lim_{t\to\infty} \boldsymbol{Q}_{ij} = [1, 0, 0, 0]^T$, $\forall(i,j) \in \mathcal{E}$.

In this section, it is required to align the orientations of all the agents. When the orientations of all the agents are aligned, the aligned local frames can be viewed as a global frame. In this global frame, the formation control problem without a global frame can be transformed into the formation control problem with a global frame.

The following auxiliary variables are defined as

$$\boldsymbol{s}_{vi}^{b} = \boldsymbol{v}_{i}^{b} - \boldsymbol{v}_{vi}^{b}, \tag{39}$$

and

$$\boldsymbol{s}_{\omega i} = \boldsymbol{\omega}_{i} - \boldsymbol{\omega}_{vi}, \tag{40}$$

where $\boldsymbol{v}_{vi}^{b} \in \mathbb{R}^3$ is a virtual velocity and $\boldsymbol{\omega}_{vi} \in \mathbb{R}^3$ denotes a virtual angular velocity.

Then, the formation control law is proposed as

$$\begin{cases} \boldsymbol{f}_{i}^{b} = -\beta_1 \boldsymbol{s}_{vi}^{b} - \beta_2 \mathrm{sig}^{r_3}\left(\boldsymbol{s}_{vi}^{b}\right) - \beta_3 \mathrm{sig}^{r_4}\left(\boldsymbol{s}_{vi}^{b}\right) - \beta_4 \mathrm{sign}\left(\boldsymbol{s}_{vi}^{b}\right) \\ \boldsymbol{v}_{vi}^{b} = -\beta_5 \sum_{j\in\mathcal{N}_i} \boldsymbol{P}(\boldsymbol{b}_{ij}^{b})\left[\boldsymbol{I}_3 + \boldsymbol{R}(\boldsymbol{Q}_{ij})\right]\boldsymbol{b}_{ij}^{b\star} \end{cases}, \tag{41a}$$

$$\begin{cases} \boldsymbol{u}_{i} = \boldsymbol{\omega}_{i}^{\times}\boldsymbol{J}_{i}\boldsymbol{\omega}_{i} - \gamma_1 \boldsymbol{s}_{\omega i} - \gamma_2 \mathrm{sig}^{r_3}(\boldsymbol{s}_{\omega i}) - \gamma_3 \mathrm{sig}^{r_4}(\boldsymbol{s}_{\omega i}) - \gamma_4 \mathrm{sign}(\boldsymbol{s}_{\omega i}) \\ \boldsymbol{\omega}_{vi} = \gamma_5 \sum_{j\in\mathcal{N}_i} \left[\boldsymbol{E}^{T}(\boldsymbol{Q}_{ij})\boldsymbol{q}_{ij} - \boldsymbol{R}(\boldsymbol{Q}_{ij})\boldsymbol{E}^{T}(\boldsymbol{Q}_{ji})\boldsymbol{q}_{ji}\right] \end{cases}, \tag{41b}$$

where β_k, γ_k, $k = 1, 2, 3, 4, 5$, $r_3 < 1$, and $r_4 > 1$ are some positive constants, $\boldsymbol{b}_{ij}^{b\star}$ is the desired bearing expressed in the body-fixed frame $\mathcal{F}_{bi}$, $\boldsymbol{E}(\boldsymbol{Q}_{ij}) = q_{0,ij}\boldsymbol{I}_3 + \boldsymbol{q}_{ij}^{\times}$, and $\boldsymbol{Q}_{ij} = [q_{0,ij}, \boldsymbol{q}_{ij}^{T}]^{T}$.

Figure 3 shows the control process under the formation control law (41). In this section, the formation control is divided into three steps. In the first step, the velocity $\boldsymbol{v}_{i}^{b}$ and the angular velocity $\boldsymbol{\omega}_{i}$ converge respectively to the designed virtual velocity $\boldsymbol{v}_{vi}^{b}$ and angular velocity $\boldsymbol{\omega}_{vi}$ in a fixed time under the control law (41). In the second step, the orientations of all agents converge to a common orientation under the control law (41b). In the third step, the inter-agent bearings $\boldsymbol{b}_{ij}^{b}$ converges to the desired bearings $\boldsymbol{b}_{ij}^{b\star}$ under the control law (41). Thus, the stability analysis of the system is also divided into these three steps.

Theorem 4. *Consider a multiagent system described by (2) and (37). If Assumptions 1 and 2 hold,* $\beta_4 \geq \beta_5 \max_{i=1,\dots,n}\{|\mathcal{N}_i|\}\left(\frac{8V_{M2}}{d_{\min}} + V_{M2} + 7V_{M3}\right) + V_{M2}V_{M3} + \epsilon_1$, $\gamma_4 \geq 10\gamma_5 V_{M3} \max_{i=1,\dots,n}\{|\mathcal{N}_i|\} + \epsilon_2$, *and the initial values satisfy* $\|\boldsymbol{v}_{i}^{b}(0)\| \leq V_{M2}$ *and* $\|\boldsymbol{\omega}_{i}(0)\| \leq V_{M3}$ *with* V_{M2} *and* V_{M3} *being positive constants, the errors* $\boldsymbol{s}_{vi}^{b}$ *and* $\boldsymbol{s}_{\omega i}$ *converge to the origin in a fixed time with a settling time* T_2 *under the control law in (41), where* T_2 *is defined as*

$$T_2 = \frac{2}{\eta_3(1 - r_3)} + \frac{2}{\eta_4(r_4 - 1)}, \tag{42}$$

with η_3 *and* η_4 *being some positive constants.*

Proof. See Appendix B. ■

Theorem 5. *If the interconnection graph is strongly connected and fixed, the attitude control law (41b) can guarantee attitude consensus, that is,* $\lim_{t\to\infty} \boldsymbol{q}_{ij} = 0, \forall i, j \in \mathcal{N}$.

Proof. See Appendix C ■

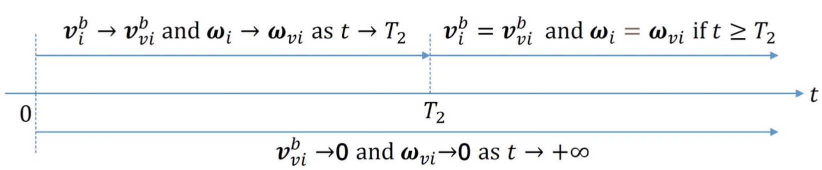

FIGURE 3 The control process under the formation control law (41).

In Theorem 4, we have proven that $\boldsymbol{v}_i^b = \boldsymbol{v}_{vi}^b$ after the time T_2. Then, the motion dynamics in (37) becomes $\dot{\boldsymbol{x}}_i = \boldsymbol{R}^T(\boldsymbol{Q}_i)\boldsymbol{v}_{vi}^b$ after the time T_2. Next, we need to prove that $\lim_{t\to\infty} \boldsymbol{b}_{ij}^b = \boldsymbol{b}_{ij}^{b\star}, \forall(i,j) \in \mathcal{E}$ under the formation control law (41). The basic idea of the proof is to prove that the formation $\mathcal{G}(\boldsymbol{x}(t))$ converges to a desired formation $\mathcal{G}(\boldsymbol{x}^\star)$.

From (41a), we have

$$\begin{aligned} \boldsymbol{R}^T(\boldsymbol{Q}_i)\boldsymbol{v}_{vi}^b &= -\beta_5 \sum_{j\in\mathcal{N}_i} \boldsymbol{R}^T(\boldsymbol{Q}_i)\boldsymbol{P}\left(\boldsymbol{b}_{ij}^b\right)\boldsymbol{R}(\boldsymbol{Q}_i)\left[\boldsymbol{R}^T(\boldsymbol{Q}_i) + \boldsymbol{R}^T\left(\boldsymbol{Q}_j\right)\right]\boldsymbol{b}_{ij}^{b\star} \\ &= -\beta_5 \sum_{j\in\mathcal{N}_i} \boldsymbol{P}(\boldsymbol{b}_{ij})\left[\boldsymbol{R}^T(\boldsymbol{Q}_i) + \boldsymbol{R}^T\left(\boldsymbol{Q}_j\right)\right]\boldsymbol{b}_{ij}^{b\star} \\ &= \underbrace{-2\beta_5 \sum_{j\in\mathcal{N}_i} \boldsymbol{P}(\boldsymbol{b}_{ij})\boldsymbol{R}^T(\boldsymbol{Q}_i)\boldsymbol{b}_{ij}^{b\star}}_{\boldsymbol{h}_i(t)} + \underbrace{\beta_5 \sum_{j\in\mathcal{N}_i} \boldsymbol{P}(\boldsymbol{b}_{ij})\left[\boldsymbol{R}(\boldsymbol{Q}_i) - \boldsymbol{R}\left(\boldsymbol{Q}_j\right)\right]^T\boldsymbol{b}_{ij}^{b\star}}_{\boldsymbol{g}_i(t)}, \end{aligned} \tag{43}$$

where the properties $\boldsymbol{b}_{ij} = \boldsymbol{R}^T(\boldsymbol{Q}_i)\boldsymbol{b}_{ij}^b$ and $\boldsymbol{P}(\boldsymbol{b}_{ij}) = \boldsymbol{R}^T(\boldsymbol{Q}_i)\boldsymbol{P}\left(\boldsymbol{b}_{ij}^b\right)\boldsymbol{R}(\boldsymbol{Q}_i)$ are applied. Denote $\boldsymbol{v}_v^b = \left[\left(\boldsymbol{v}_{v1}^b\right)^T, \dots, \left(\boldsymbol{v}_{vn}^b\right)^T\right]^T$, $\boldsymbol{h}(t) = \left[\boldsymbol{h}_1^T(t), \dots, \boldsymbol{h}_n^T(t)\right]^T$, and $\mathbf{g}(t) = \left[\mathbf{g}_1^T(t), \dots, \mathbf{g}_n^T(t)\right]^T$. Then, we have

$$\operatorname{diag}\left(\boldsymbol{R}^T(\boldsymbol{Q}_i)\right)\boldsymbol{v}_v^b = \boldsymbol{h}(t) + \mathbf{g}(t). \tag{44}$$

Theorem 6. *Given the multiagent systems described by (2) and (37), the errors $\boldsymbol{x}_e = \boldsymbol{x} - \boldsymbol{x}^\star$ converge asymptotically to $\boldsymbol{x}_e = \mathbf{0}$ under the control law (41).*

Proof. Choose the Lyapunov function as

$$V_{x_e} = \frac{1}{2}\|\boldsymbol{x}_e\|^2. \tag{45}$$

Substituting (44) into $\dot{V}_{x_e}$ yields

$$\begin{aligned} \dot{V}_{x_e} &= \left(\boldsymbol{x} - \boldsymbol{x}^\star\right)^T\dot{\boldsymbol{x}} \\ &= \left(\boldsymbol{x} - \boldsymbol{x}^\star\right)^T\operatorname{diag}\left(\boldsymbol{R}^T(\boldsymbol{Q}_i)\right)\boldsymbol{v}^b \\ &= \left(\boldsymbol{x} - \boldsymbol{x}^\star\right)^T\operatorname{diag}\left(\boldsymbol{R}^T(\boldsymbol{Q}_i)\right)\left(\boldsymbol{v}_v^b + \boldsymbol{s}_v^b\right) \\ &= -\left(\boldsymbol{x}^\star\right)^T\operatorname{diag}\left(\boldsymbol{R}^T(\boldsymbol{Q}_i)\right)\boldsymbol{v}_v^b + \boldsymbol{x}_e^T\operatorname{diag}\left(\boldsymbol{R}^T(\boldsymbol{Q}_i)\right)\boldsymbol{s}_v^b \\ &= \underbrace{-\left(\boldsymbol{x}^\star\right)^T\boldsymbol{h}(t) + \boldsymbol{x}_e^T\operatorname{diag}\left(\boldsymbol{R}^T(\boldsymbol{Q}_i)\right)\boldsymbol{s}_v^b}_{\boldsymbol{z}(t)} - \left(\boldsymbol{x}^\star\right)^T\mathbf{g}(t), \end{aligned} \tag{46}$$

where $\boldsymbol{v}^b = \left[\left(\boldsymbol{v}_1^b\right)^T, \dots, \left(\boldsymbol{v}_n^b\right)^T\right]^T$, $\boldsymbol{s}_v^b = \left[\left(\boldsymbol{s}_{v1}^b\right)^T, \dots, \left(\boldsymbol{s}_{vn}^b\right)^T\right]^T$, and the property $\boldsymbol{R}^T(\boldsymbol{Q}_i)\boldsymbol{v}_{vi}^b \perp \operatorname{span}\{\boldsymbol{x}_i\}$ Reference 22(Lemma 9) is applied.

The proof is divided into two phases: $t \in [0, T_2)$ and $t \in [T_2, \infty)$, where T_2 is defined in (42). In the phase $t \in [0, T_2)$, we prove that $\boldsymbol{x}_e$ is bounded. In the phase $t \in [T_2, \infty)$, we prove that the equilibrium $\boldsymbol{x}_e = 0$ is almost globally asymptotically stable.

Phase $t \in [0, T_2)$: Similar with the proof of Theorem 2, we have

$$\boldsymbol{z}(t) \leq -\mu_2\lambda_5 V_{x_e} + \frac{\|\boldsymbol{s}_v^b(0)\|^2}{2\mu_2\lambda_5}, \tag{47}$$

where $\mu_2 = \frac{\beta_5 \min_{k=1,\dots,m}\|\boldsymbol{e}_k^\star\|}{(\sqrt{2}\|\boldsymbol{x}(0)\| + \sqrt{2}T_1\|\boldsymbol{s}_v^b(0)\| + 2T_1 n\alpha_5)^2}$, λ_5 is the minimum positive eigenvalue of $\overline{\boldsymbol{\Gamma}}^T\left(\boldsymbol{x}^\star\right)\overline{\boldsymbol{\Gamma}}\left(\boldsymbol{x}^\star\right)$, and $\overline{\boldsymbol{\Gamma}}\left(\boldsymbol{x}^\star\right)$ is defined in (24). Then, Substituting (47) into (46) yields

$$\begin{aligned} \dot{V}_{x_e} &\leq -\mu_2\lambda_5 V_{x_e} + \frac{\|\boldsymbol{s}_v^b(0)\|^2}{2\mu_2\lambda_5} + \|\boldsymbol{x}^\star\|\|\mathbf{g}(t)\| \\ &\leq -\mu_2\lambda_5 V_{x_e} + \frac{\|\boldsymbol{s}_v^b(0)\|^2}{2\mu_2\lambda_5} + 2n\beta_5\sum_{i=1}^n |\mathcal{N}_i|\|\boldsymbol{x}^\star\|, \end{aligned} \tag{48}$$

where the fact that $\|\boldsymbol{g}(t)\| \leq 2n\beta_5 \max_{i\in\mathcal{V}}\{|\mathcal{N}_i|\}$ is applied. Thus, $\boldsymbol{x}_e$ is bounded during $t \in [0, T_2)$.

Phase $t \in [T_2, \infty)$: It follows from Theorem 4 that $\boldsymbol{v}_i^b = \boldsymbol{v}_{vi}^b$ and $\boldsymbol{\omega}_i = \boldsymbol{\omega}_{vi}$ after the time T_2. Similar with the proof of Theorem 2, we have

$$\boldsymbol{z}(t) \leq -2\mu_2\lambda_5 V_{x_e}. \tag{49}$$

Then, Substituting (49) into (46) yields

$$\dot{V}_{x_e} \leq -2\mu_2\lambda_5 V_{x_e} + \|\boldsymbol{x}^\star\|\|\mathbf{g}(t)\|. \tag{50}$$

It follows from Theorem 5 that $\boldsymbol{Q}_i \to \boldsymbol{Q}_j, \forall i,j \in \mathcal{V}$ as $t \to \infty$, which implies that $\lim_{t\to\infty} \|\boldsymbol{g}(t)\| = 0$. Thus, it can be concluded from Reference 41(Proposition 2) that the system is almost globally input-to-state stability. The equilibrium $\boldsymbol{x}_e = 0$ is almost globally asymptotically stable. ■

4.2 | Collision avoidance

The control law (41) cannot guarantee that no agent collides with its neighbors. If two agents collide, the stability result of Theorem 4 may be invalid. In this section, a sufficient condition is provided to guarantee that each agent maintains a minimum distance with its neighbors under the formation control law (41).

Theorem 7. *Under Assumption 1 and the formation control law (41), if the initial states $\boldsymbol{x}_e(0)$ and $\boldsymbol{s}_v^b(0)$ satisfy*

$$\|\boldsymbol{x}_e(0)\| < \frac{1}{\sqrt{n}}\left(\min_{i,j\in\mathcal{V}} \|\boldsymbol{x}_i^\star - \boldsymbol{x}_j^\star\| - d_{\min}\right), \tag{51}$$

and

$$\|\boldsymbol{s}_v^b(0)\| < \sqrt{\left[\lambda_5\mu_2\left(\min_{i,j\in\mathcal{V}} \|\boldsymbol{x}_i^\star - \boldsymbol{x}_j^\star\| - d_{\min}\right)\right]^2 - 4n\beta_5\lambda_5\mu_2\sum_{i=1}^{n}|\mathcal{N}_i|\|\boldsymbol{x}^\star\|}, \tag{52}$$

where λ_5 is the minimum positive eigenvalue of $\overline{\boldsymbol{\Gamma}}^T(\boldsymbol{x}^\star)\overline{\boldsymbol{\Gamma}}(\boldsymbol{x}^\star)$, and $\overline{\boldsymbol{\Gamma}}(\boldsymbol{x}^\star)$ is defined in (24), then it can be guaranteed that

$$\|\boldsymbol{x}_i(t) - \boldsymbol{x}_j(t)\| > d_{\min} > 0, \forall i,j \in \mathcal{V}, \forall t \geq 0.$$

Proof. The proof is similar with the proof of Theorem 3 and is omitted. ■

Remark 2. It should be pointed out that the conditions in Theorem 3 and 7 are conservative. Extensive simulations verify that the collisions may be avoided under the formation control laws (14) and (41) even if the proposed conditions do not hold.

Remark 3. The proposed control laws are distributed such that each agent just needs to obtain the relative measurements with respect to its neighbors. Thus, the computation scales with the number of neighbors, which is generally much smaller than the total number of agents.

5 | SIMULATION EXAMPLES

In this section, some simulation examples are provided to demonstrate the effectiveness of the control schemes in (14) and (41).

5.1 | Simulation for bearing formation control with a global inertial frame

In this subsection, two simulation examples where the desired formations are shown respectively in Figure 4A,B are provided to illustrate the control law (14). It can be observed that these desired frameworks in Figure 4A,B are IBR and not IBR, respectively. The example without an IBR desired framework is to verify the necessity of Assumption 1. The disturbances in the dynamics of agent i are assumed as $\boldsymbol{\Delta}_i = -5\sin\left(\frac{t}{10}\right)\mathbf{1}_3\ m/s^2, \forall i = 1, 2, \ldots, 8$.

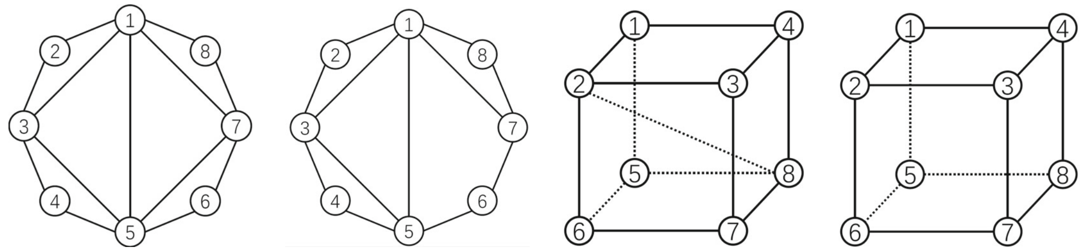

(A) A ring with $|\mathcal{E}| = 26$. (B) A ring with $|\mathcal{E}| = 24$. (C) A cube with $|\mathcal{E}| = 26$. (D) A cube with $|\mathcal{E}| = 24$.

FIGURE 4 Desired formations for simulation examples.

TABLE 1 Simulation parameters for the example under the control law (14).

Name	Value
The initial positions of agents (m)	$\boldsymbol{x}_1(0) = [148.1,\ 406.9,\ 400]^T,\ \boldsymbol{x}_2(0) = [0,\ 433,\ 350]^T,$
	$\boldsymbol{x}_3(0) = [-406.9,\ 148.1,\ 300]^T,\ \boldsymbol{x}_4(0) = [-433,\ 0,\ 250]^T,$
	$\boldsymbol{x}_5(0) = [-148.1,\ -406.9,\ 300]^T,\ \boldsymbol{x}_6(0) = [0,\ -433,\ 350]^T,$
	$\boldsymbol{x}_7(0) = [406.9,\ -148.1,\ 400]^T,\ \boldsymbol{x}_8(0) = [433,\ 0,\ 450]^T.$
The initial velocities of agents (m/s)	$\boldsymbol{v}_i(0) = [0,\ 0,\ 0]^T,\ i = 1, \dots, 8.$
The desired bearings	$\boldsymbol{b}^\star_{12} = [-0.9239,\ 0.3827,\ 0]^T,\ \boldsymbol{b}^\star_{13} = [-1,\ 0,\ 0]^T,$
	$\boldsymbol{b}^\star_{17} = [0,\ -1,\ 0]^T,\ \boldsymbol{b}^\star_{18} = [0.3827,\ -0.9239,\ 0]^T,$
	$\boldsymbol{b}^\star_{23} = [-0.9239,\ -0.3827,\ 0]^T,\ \boldsymbol{b}^\star_{34} = [-0.3827,\ -0.9239,\ 0]^T,$
	$\boldsymbol{b}^\star_{35} = [0,\ -1,\ 0]^T,\ \boldsymbol{b}^\star_{45} = [0.3827,\ -0.9239,\ 0]^T,$
	$\boldsymbol{b}^\star_{56} = [0.9239,\ -0.3827,\ 0]^T,\ \boldsymbol{b}^\star_{57} = [1,\ 0,\ 0]^T,$
	$\boldsymbol{b}^\star_{67} = [0.9239,\ 0.3827,\ 0]^T,\ \boldsymbol{b}^\star_{78} = [0.3827,\ 0.9239,\ 0]^T.$
	The other bearings can be calculated by $\boldsymbol{b}^\star_{ij} = -\boldsymbol{b}^\star_{ji}$.
The control parameters	$\alpha_1 = 0.2,\ \alpha_2 = 1,\ \alpha_3 = 0.2,\ \alpha_4 = 0.005,\ \alpha_5 = 0.3.$

The simulation parameters of the two examples are chosen as the same and are given in Table 1. As shown in Figure 5, the initial and final positions of agents are drawn in gray and red dots, respectively. The initial and final sensing graphs are plotted in gray and red lines, respectively. The trajectories of agents are represented by the gray dash lines. Figure 6 shows the equivalent bearing errors $\sum_{(i,j)\in\mathcal{E}} \|\boldsymbol{b}_{ij} - \boldsymbol{b}^\star_{ij}\|$ and total bearing errors $\sum_{i=1}^{n}\sum_{j=1}^{n} \|\boldsymbol{b}_{ij} - \boldsymbol{b}^\star_{ij}\|$ of the two examples under the control law (14). It can be observed from Figure 5 and 6A that the agents are steered to the formations that have the same bearings with the desired formations in two examples. However, it can be observed from Figure 6B that the final framework in the example without IBR desired framework is not the desired framework since the desired framework is not unique. This verifies the necessity of Assumption 1. Figure 7 shows the trajectory of the formation scale l defined in (17) in the example with IBR desired formation. The velocities and virtual velocities of agents in the example with IBR desired formation are shown in Figures 8 and 9, respectively. The velocities of agents can track the virtual velocities in just 5 seconds under the control law (14). The control inputs of agents in the example with IBR desired formation are plotted in Figure 10. It can be observed that the control forces do not reach zero due to the effect of disturbances. This yields that the formation scale floats around a value. Due to space constraint, the trajectories of the formation scale l, the velocities, virtual velocities, and control forces in the example without IBR desired formation are omitted.

5.2 | Simulation for bearing formation control without a global inertial frame

In this subsection, two examples where the desired formations are shown respectively in Figure 4C,D are provided to illustrate the control law (41). Differing from the example in the previous subsection, the agents can only measure the

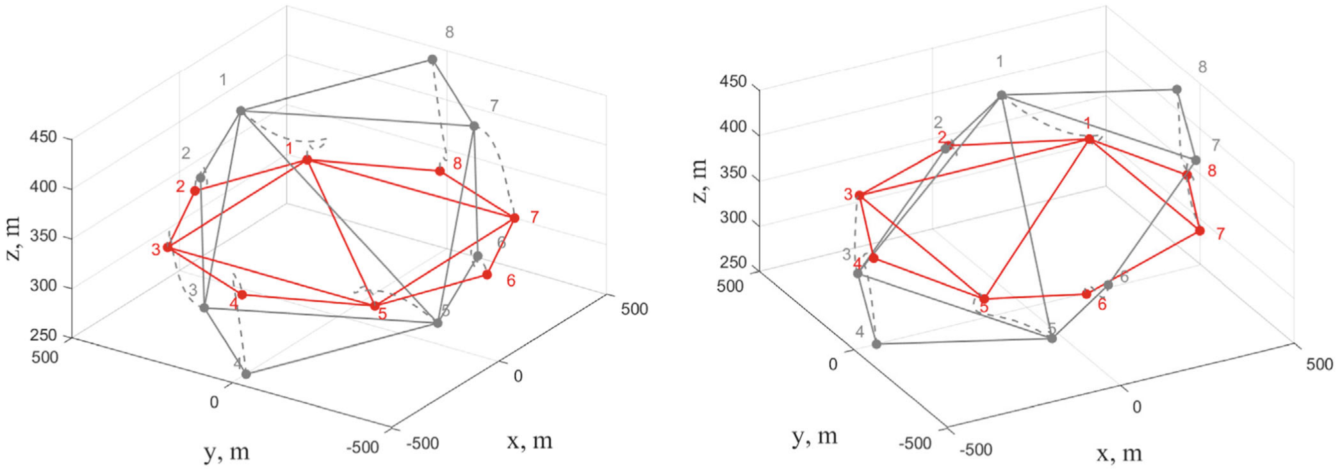

(A) The example with IBR desired formation.
(B) The example without IBR desired formation.

FIGURE 5 The examples under the control law (14).The initial and final formations are marked in gray and red, respectively. The trajectories of all agents are drawn in gray dash line.

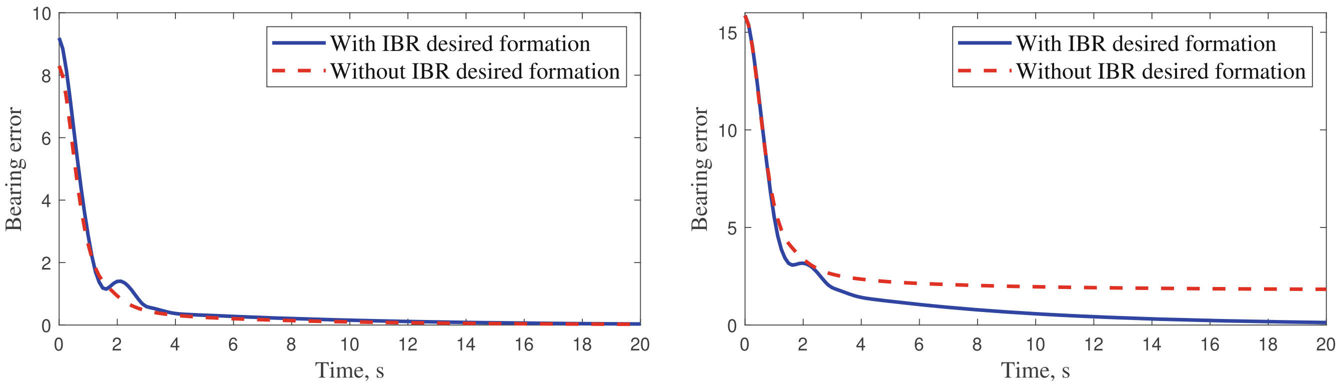

(A) The equivalent bearing errors.
(B) The total bearing error.

FIGURE 6 The equivalent bearing errors $\sum_{(i,j)\in\mathcal{E}} \|\boldsymbol{b}_{ij} - \boldsymbol{b}_{ij}^{\star}\|$ and total bearing $\sum_{i=1}^{n}\sum_{j=1}^{n} \|\boldsymbol{b}_{ij} - \boldsymbol{b}_{ij}^{\star}\|$ under the control law (14).

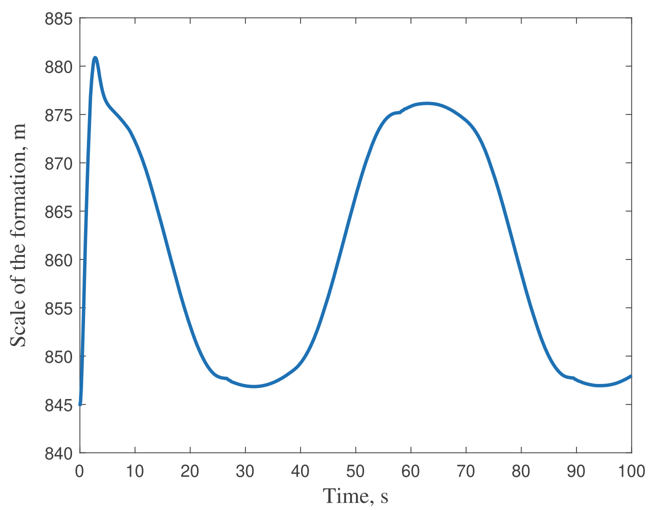

FIGURE 7 The formation scale l in the example with IBR desired formation under the control law (14).

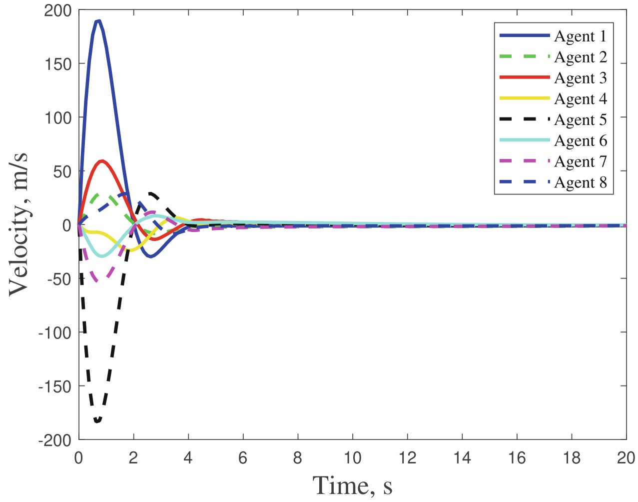

(A) The velocities $v_{i,1}$.

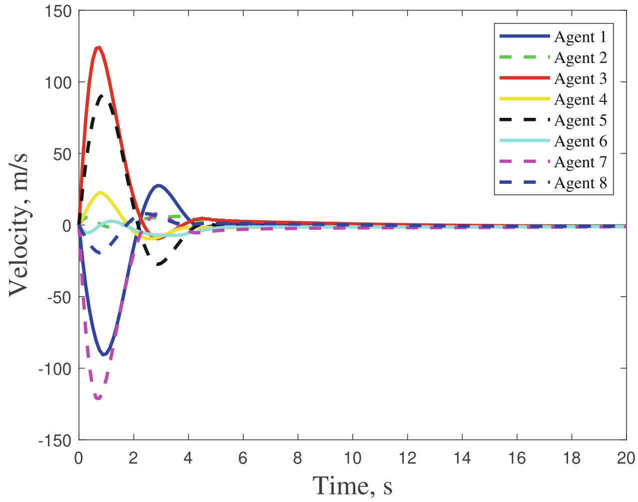

(B) The velocities $v_{i,2}$.

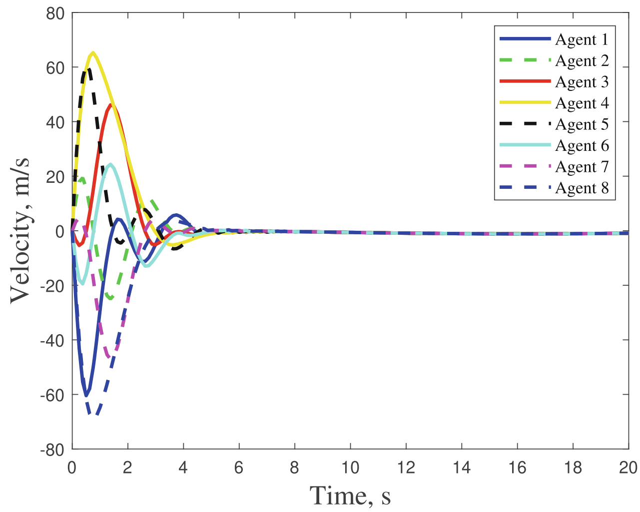

(C) The velocities $v_{i,3}$.

FIGURE 8 The velocities $\boldsymbol{v}_i = [v_{i,1}, v_{i,2}, v_{i,3}]^T$ in the example with IBR desired formation under the control law (14).

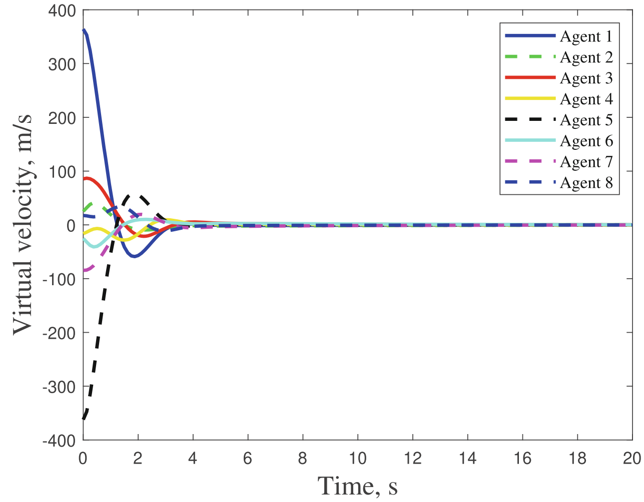

(A) The virtual velocities $v_{vi,1}$.

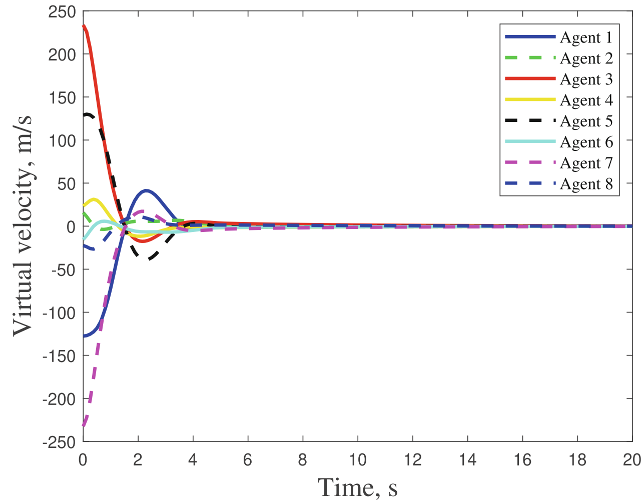

(B) The virtual velocities $v_{vi,2}$.

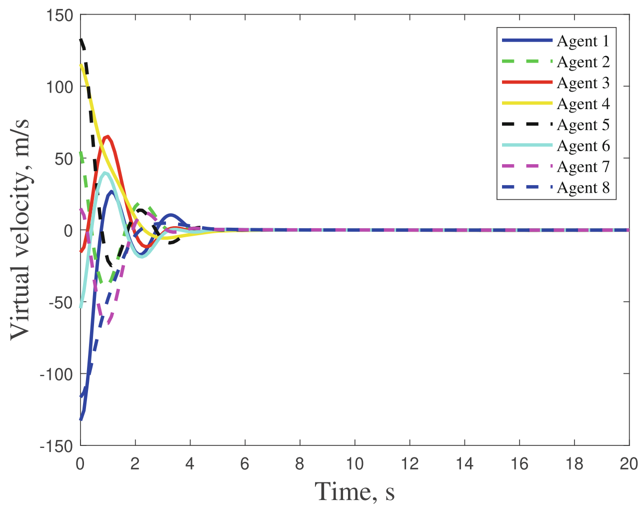

(C) The virtual velocities $v_{vi,3}$.

FIGURE 9 The virtual velocities $\boldsymbol{v}_{vi} = [v_{vi,1}, v_{vi,2}, v_{vi,3}]^T$ in the example with IBR desired formation under the control law (14).

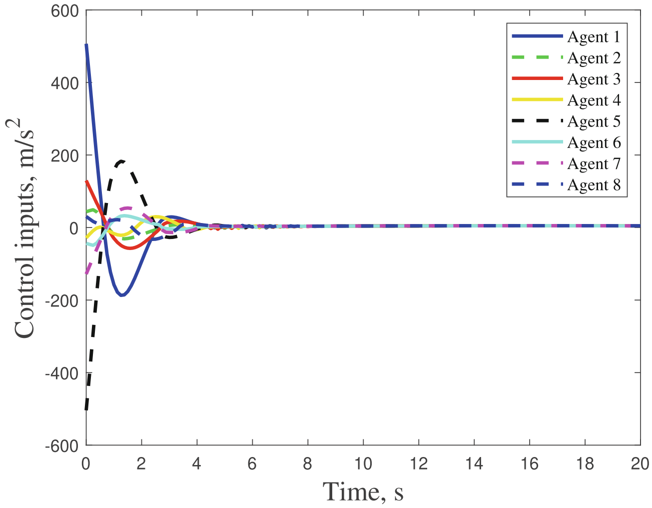

(A) Control forces $f_{i,1}$.

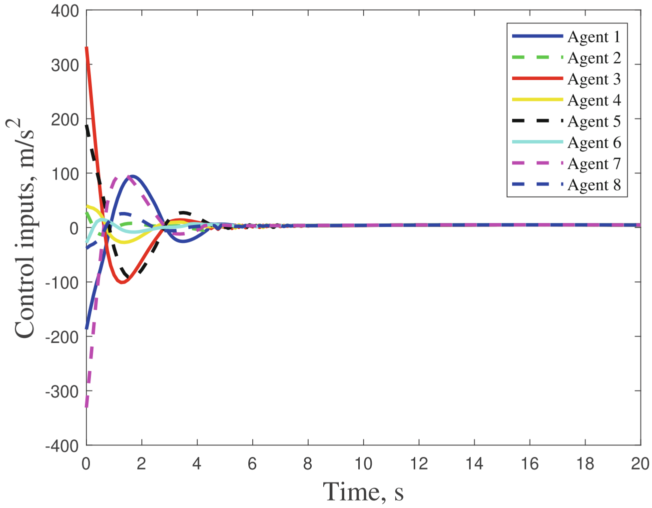

(B) Control forces $f_{i,2}$.

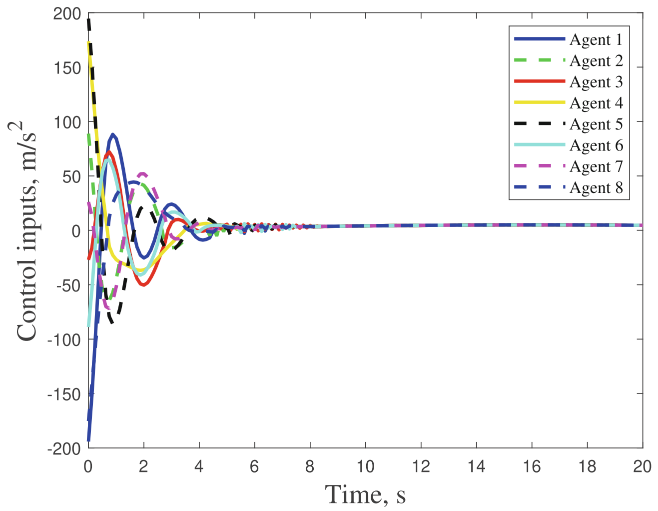

(C) Control forces $f_{i,3}$.

FIGURE 10 The control forces $\boldsymbol{f}_i = [f_{i,1}, f_{i,2}, f_{i,3}]^T$ in the example with IBR desired formation under the control law (14).

bearings in the body-fixed frame in this example, and the desired formation is a cube. The desired framework in Figure 4C is IBR, and desired framework in Figure 4D is not IBR. The disturbance in the dynamics of agent i is also assumed as $\boldsymbol{\Delta}_i = -5\sin\left(\frac{t}{10}\right)\mathbf{1}_3\ m/s^2, \forall i = 1, 2, \dots, 8$.

In this subsection, the initial positions and velocities of agents are chosen as the same with those in the previous subsection. The other parameters of agents are given in Table 2. As shown in Figure 11, the initial and final positions of agents are drawn in gray and red dots, respectively. The initial and final sensing graphs are plotted in gray and red lines, respectively. The trajectories of agents are represented by the gray dash lines. The short blue lines represent the orientations of agents. Figure 12 shows the equivalent bearing errors $\sum_{(i,j)\in\mathcal{E}} \|\boldsymbol{b}_{ij} - \boldsymbol{b}_{ij}^{\star}\|$ and total bearing error $\sum_{i=1}^{n}\sum_{j=1}^{n} \|\boldsymbol{b}_{ij} - \boldsymbol{b}_{ij}^{\star}\|$ of the two examples under the control law (41). It can be observed that the final framework in the example with IBR desired formation is the same with that in Figure 4C, but the final framework in the example without IBR desired formation is different with that in Figure 4D. Figure 13 shows the attitude consensus error $\sum_{(i,j)\in\mathcal{E}} \|\boldsymbol{\Theta}(\boldsymbol{Q}_i) - \boldsymbol{\Theta}(\boldsymbol{Q}_j)\|$ in the example with IBR desired formation under the control law (41). It can be observed from Figure 13 that the orientation of each agent finally synchronizes. Figure 14 shows the trajectory of the formation scale l defined in (41) in the example with IBR desired formation. The velocities and virtual velocities of agents in the example with IBR desired formation are shown in Figures 15 and 16, respectively. Figures 17 and 18 show the angular velocities and virtual angular velocity, respectively,

TABLE 2 Simulation parameters for the example under the control law (41).

Name	Value
The initial orientations of agents	$\boldsymbol{Q}_1(0) = [0.926,\ 0.35,\ -0.1,\ -0.1]^T$, $\boldsymbol{Q}_2(0) = [0.9055,\ -0.1,\ 0.1,\ 0.4]^T$, $\boldsymbol{Q}_3(0) = [0.9747,\ 0,\ -0.2,\ -0.1]^T$, $\boldsymbol{Q}_4(0) = [0.5172,\ -0.1,\ 0,\ 0.85]^T$, $\boldsymbol{Q}_5(0) = [0.8,\ 0,\ 0.6,\ 0]^T$, $\boldsymbol{Q}_6(0) = [0.6614,\ 0.75,\ 0,\ 0]^T$, $\boldsymbol{Q}_7(0) = [0.9887,\ 0,\ 0,\ -0.15]^T$, $\boldsymbol{Q}_8(0) = [0.926,\ -0.1,\ -0.1,\ -0.35]^T$.
The initial angular velocities of agents	$\boldsymbol{\omega}_i(0) = [0,\ 0,\ 0]^T$ deg/s, $i = 1, \dots, 8$.
The inertia matrices of agents	$\boldsymbol{J}_i(0) = [145,\ 7,\ 6;\ 6,\ 150,\ 8;\ 6,\ 8,\ 155]^T$ kg·m^2, $i = 1, \dots, 8$.
The desired bearings	$\boldsymbol{b}^\star_{12} = [-1,\ 0,\ 0]^T$, $\boldsymbol{b}^\star_{14} = [0,\ -1,\ 0]^T$, $\boldsymbol{b}^\star_{15} = [0,\ 0,\ -1]^T$, $\boldsymbol{b}^\star_{23} = [0,\ -1,\ 0]^T$, $\boldsymbol{b}^\star_{26} = [0,\ 0,\ -1]^T$, $\boldsymbol{b}^\star_{28} = [0.5774,\ -0.5774,\ -0.5774]^T$, $\boldsymbol{b}^\star_{34} = [1,\ 0,\ 0]^T$, $\boldsymbol{b}^\star_{37} = [0,\ 0,\ 1]^T$, $\boldsymbol{b}^\star_{48} = [0,\ 0,\ -1]^T$, $\boldsymbol{b}^\star_{56} = [-1,\ 0,\ 0]^T$, $\boldsymbol{b}^\star_{58} = [0,\ -1,\ 0]^T$, $\boldsymbol{b}^\star_{67} = [0,\ -1,\ 0]^T$, $\boldsymbol{b}^\star_{78} = [1,\ 0,\ 0]^T$. The other bearings can be calculated by $\boldsymbol{b}^\star_{ij} = -\boldsymbol{b}^\star_{ji}$.
The control parameters	$\beta_1 = 2,\ \beta_2 = 0.2,\ \beta_3 = 1,\ \beta_4 = 0.001,\ \beta_5 = 0.1$, $\gamma_1 = 100,\ \gamma_2 = 10,\ \gamma_3 = 1,\ \gamma_4 = 0.01,\ \gamma_5 = 0.1$.

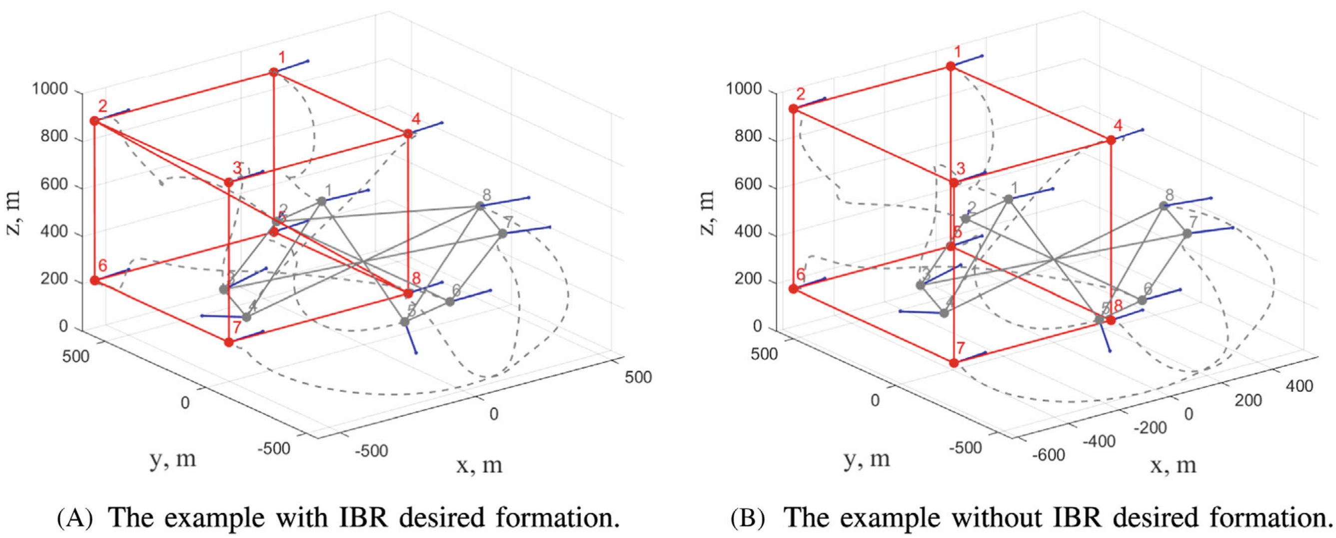

FIGURE 11 The example under the control law (41). The initial and final formations are marked in gray and red, respectively. The orientations of agents are marked in blue. The trajectories of all agents are drawn in gray dash line.

in the example with IBR desired formation. It is found that the velocities and angular velocities of agents can converge to the virtual velocities and angular velocity in just a few seconds, respectively. The control forces and control torques of agents in the example with IBR desired formation are plotted in Figures 19 and 20, respectively. Due to space constraint, the other trajectories in the example without IBR desired formation are omitted.

In this simulation, a comparison between the proposed bearing-based formation control law (41) and the bearing-based formation control law in Reference 42 is conducted to verify the disturbance rejection ability of the proposed control law. The formation control law in Reference 42 does not take the disturbances into consideration. The initial states are chosen as the same with those in Table 2. Figure 21 shows the equivalent bearing errors $\sum_{(i,j)\in\mathcal{E}} \|\boldsymbol{b}_{ij} - \boldsymbol{b}^\star_{ij}\|$ between the proposed bearing-based formation control law (41) and the bearing-based formation control law in Reference 42. It can be observed from Figure 21 that the equivalent bearing error under the formation control law (41) is smaller than those under the formation control law in Reference 42. This verifies the disturbance rejection ability of the proposed control law.

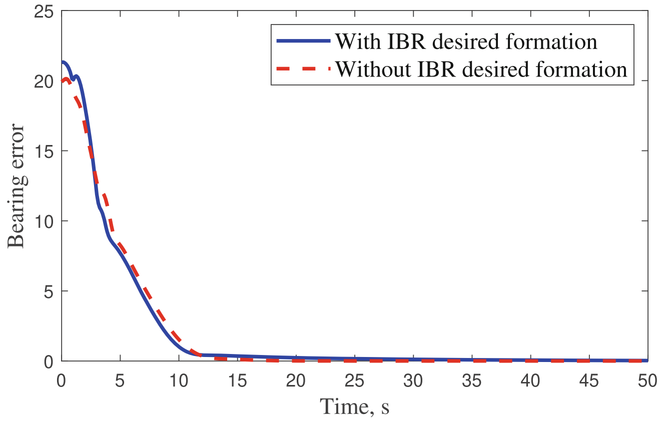

(A) The equivalent bearing errors.

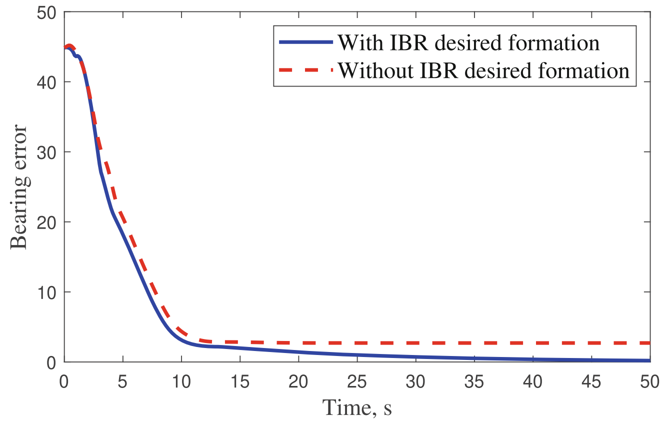

(B) The total bearing error.

FIGURE 12 The equivalent bearing errors $\sum_{(i,j)\in\mathcal{E}} \|\boldsymbol{b}_{ij} - \boldsymbol{b}_{ij}^{\star}\|$ and total bearing error $\sum_{i=1}^{n}\sum_{j=1}^{n}\|\boldsymbol{b}_{ij} - \boldsymbol{b}_{ij}^{\star}\|$ under the control law (41).

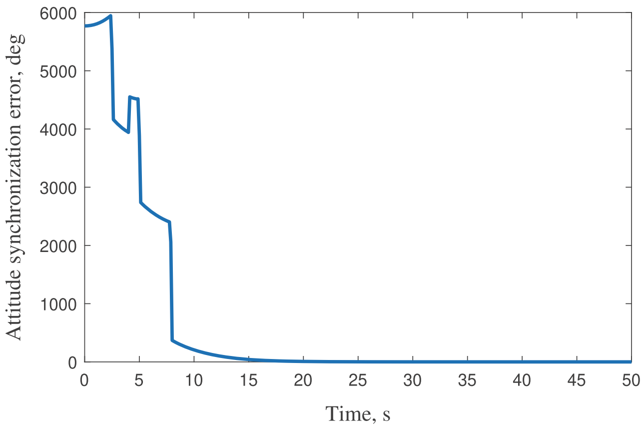

FIGURE 13 The attitude consensus error $\sum_{(i,j)\in\mathcal{E}} \|\boldsymbol{\Theta}(\boldsymbol{Q}_i) - \boldsymbol{\Theta}(\boldsymbol{Q}_j)\|$ in the example with IBR desired formation under the control law (41). $\boldsymbol{\Theta}(\boldsymbol{Q})$ is the Euler angles converted by $\boldsymbol{Q}$.

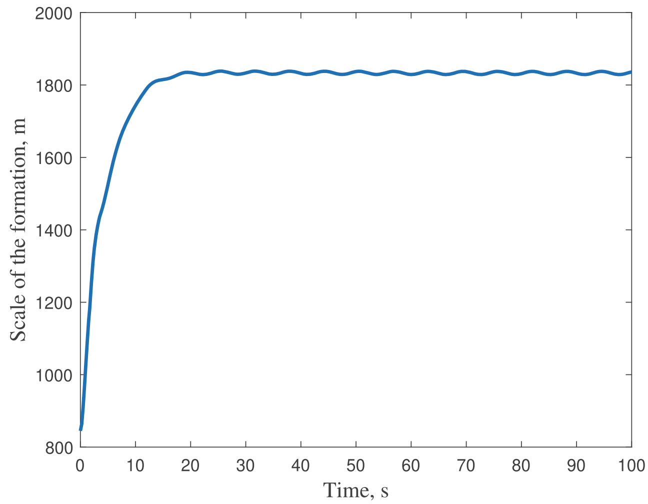

FIGURE 14 The formation scale l in the example with IBR desired formation under the control law (41).

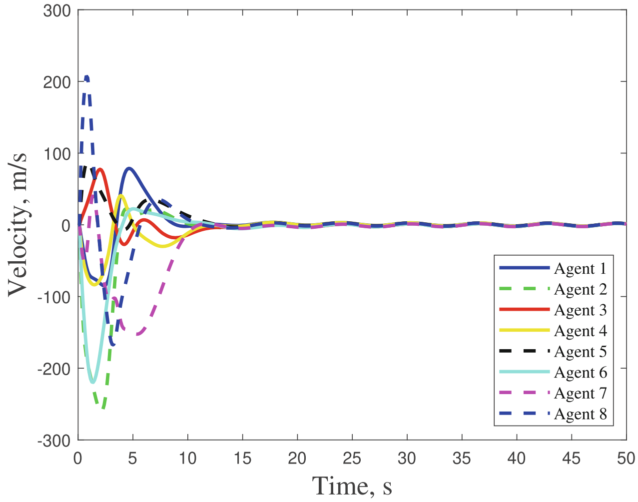

(A) The velocities $v_{i,1}^b$.

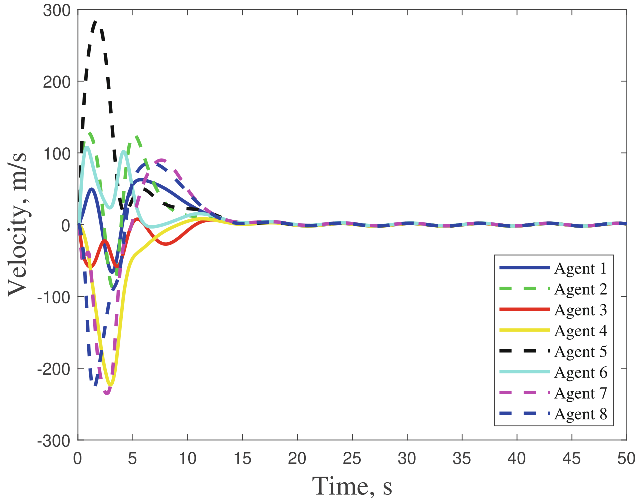

(B) The velocities $v_{i,2}^b$.

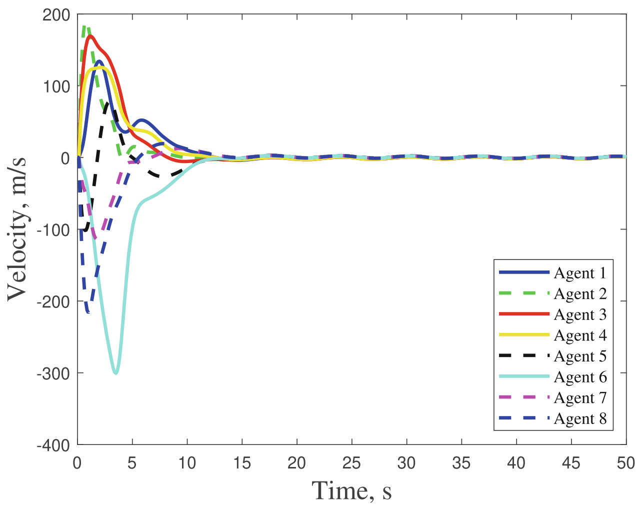

(C) The velocities $v_{i,3}^b$.

FIGURE 15 The velocities $\boldsymbol{v}_i^b = [v_{i,1}^b, v_{i,2}^b, v_{i,3}^b]^T$ in the example with IBR desired formation under the control law (41a).

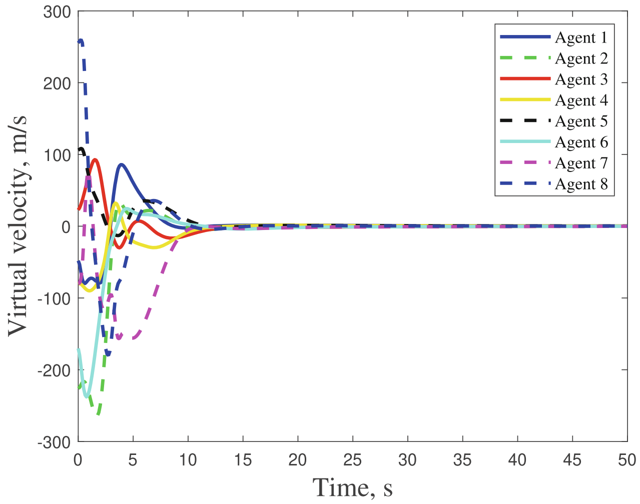

(A) The velocities $v^b_{vi,1}$.

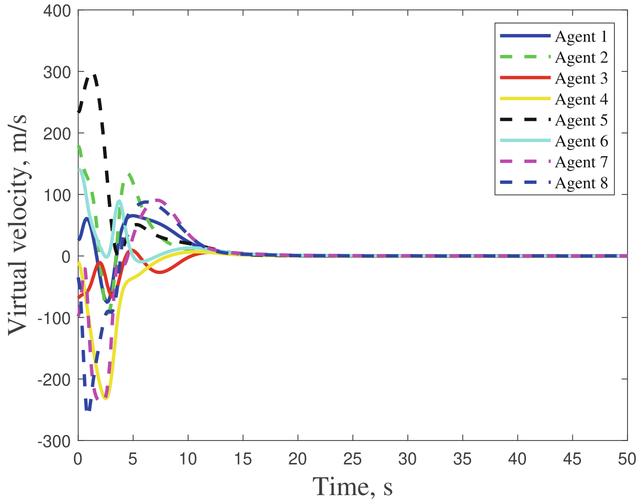

(B) The virtual velocities $v^b_{vi,2}$.

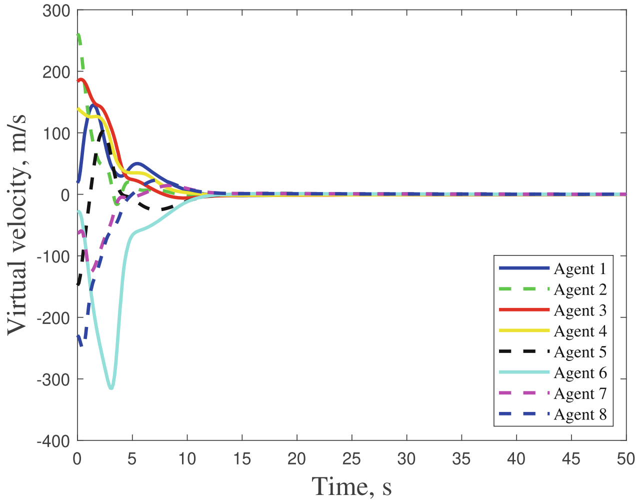

(C) The virtual velocities $v^b_{vi,3}$.

FIGURE 16 The virtual velocities $\boldsymbol{v}^b_{vi} = [v^b_{vi,1}, v^b_{vi,2}, v^b_{vi,3}]^T$ in the example with IBR desired formation under the control law (41a).

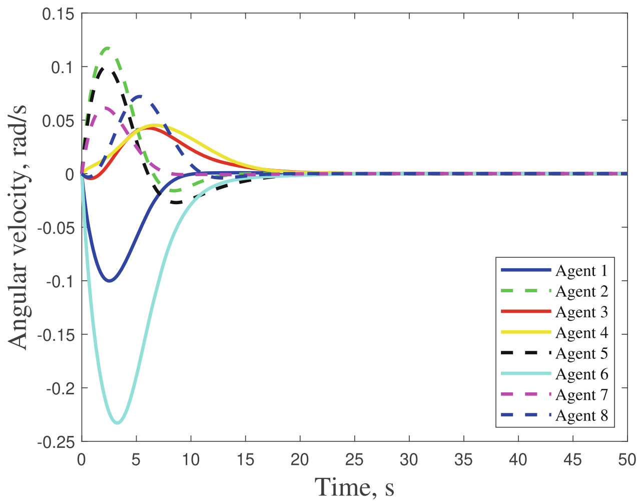

(A) The angular velocities $\omega_{i,1}$.

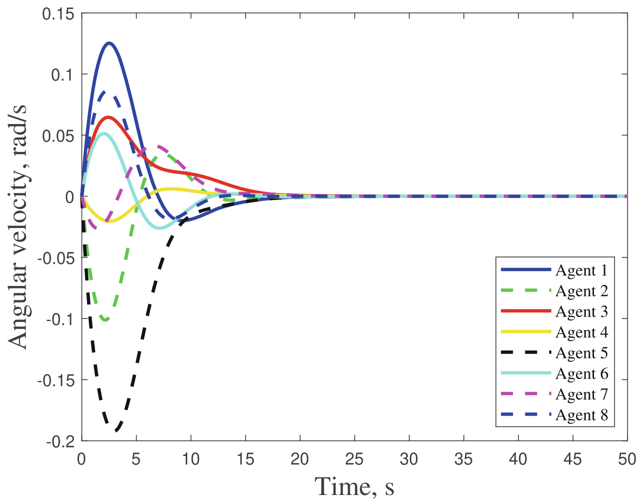

(B) The angular velocities $\omega_{i,2}$.

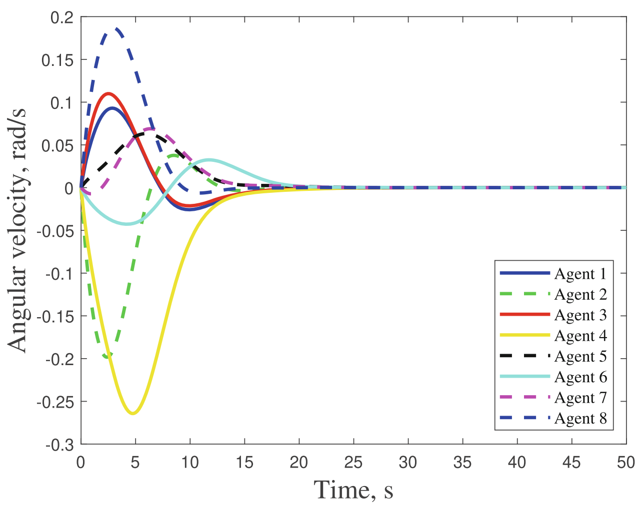

(C) The angular velocities $\omega_{i,3}$.

FIGURE 17 The angular velocities $\boldsymbol{\omega}_i = [\omega_{i,1}, \omega_{i,2}, \omega_{i,3}]^T$ in the example with IBR desired formation under the control law (41b).

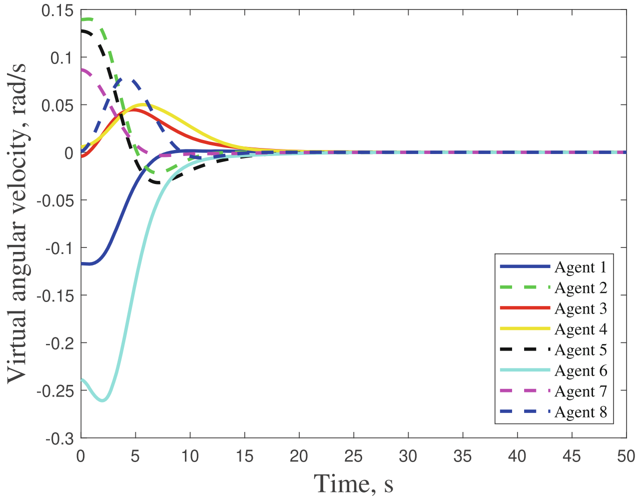

(A) The virtual angular velocities $\omega_{vi,1}$.

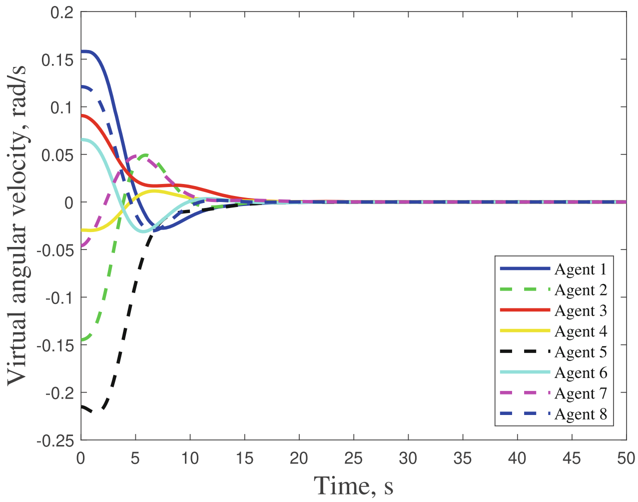

(B) The virtual angular velocities $\omega_{vi,2}$.

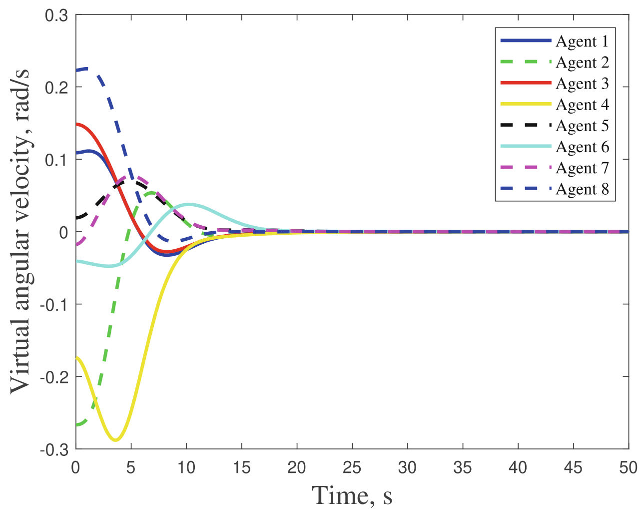

(C) The virtual angular velocities $\omega_{vi,3}$.

FIGURE 18 The virtual angular velocities $\boldsymbol{\omega}_{vi} = [\omega_{vi,1}, \omega_{vi,2}, \omega_{vi,3}]^T$ in the example with IBR desired formation under the control law (41b).

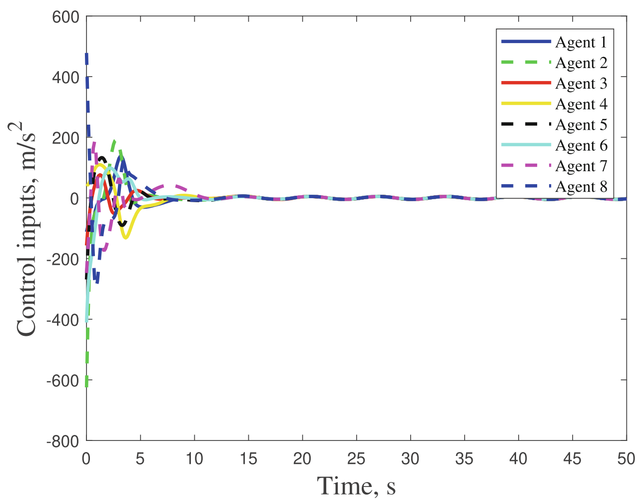

(A) Control inputs $f^b_{i,1}$.

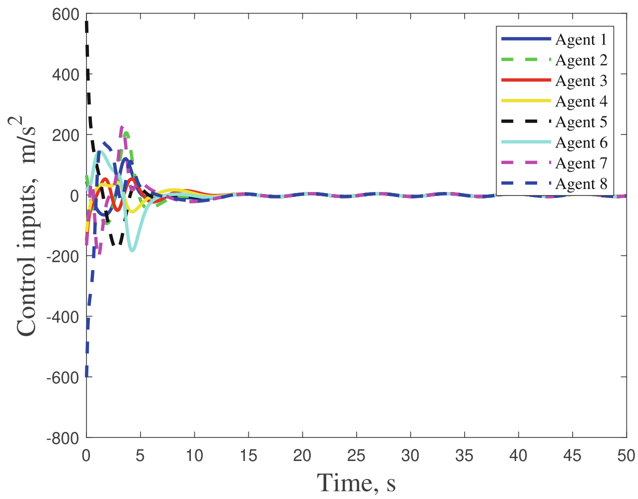

(B) Control inputs $f^b_{i,2}$.

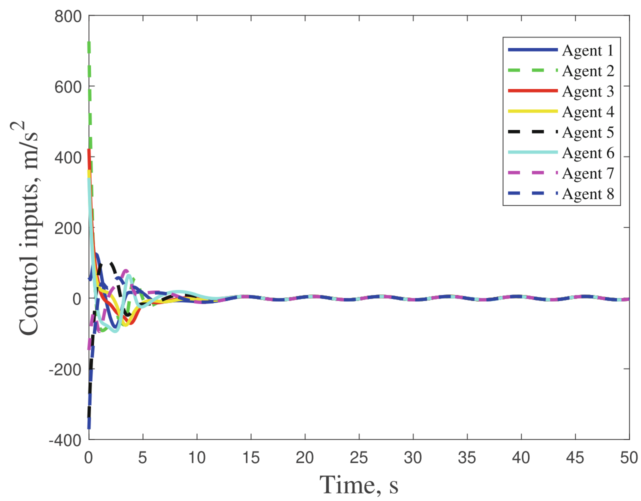

(C) Control inputs $f^b_{i,3}$.

FIGURE 19 The control inputs $\boldsymbol{f}^b_i = [f^b_{i,1}, f^b_{i,2}, f^b_{i,3}]^T$ in the example with IBR desired formation under the control law (41a).

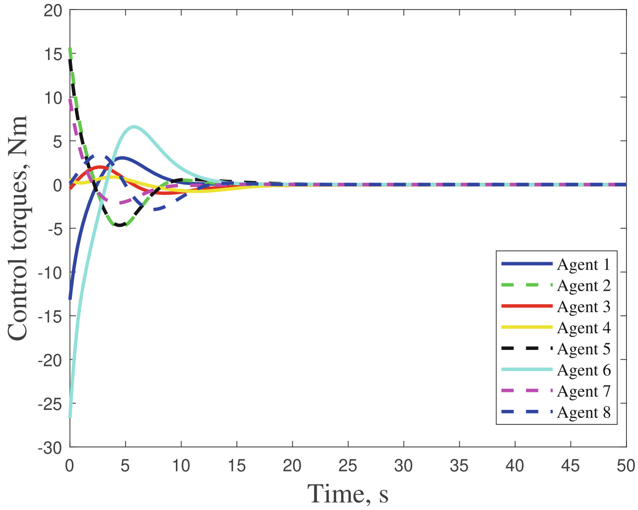

(A) The control torques $u_{i,1}$.

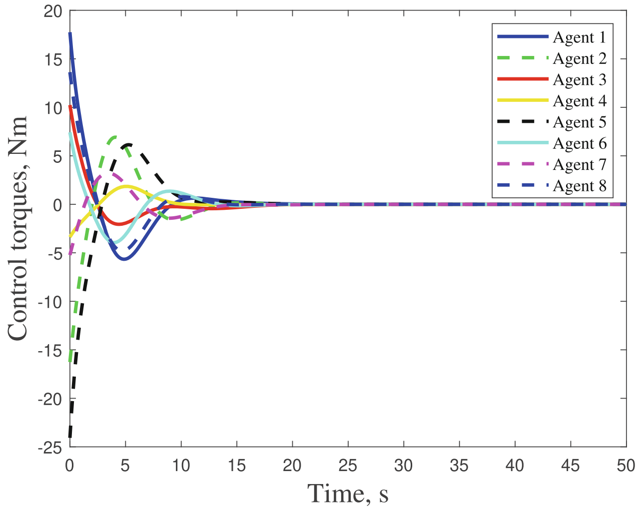

(B) The control torques $u_{i,2}$.

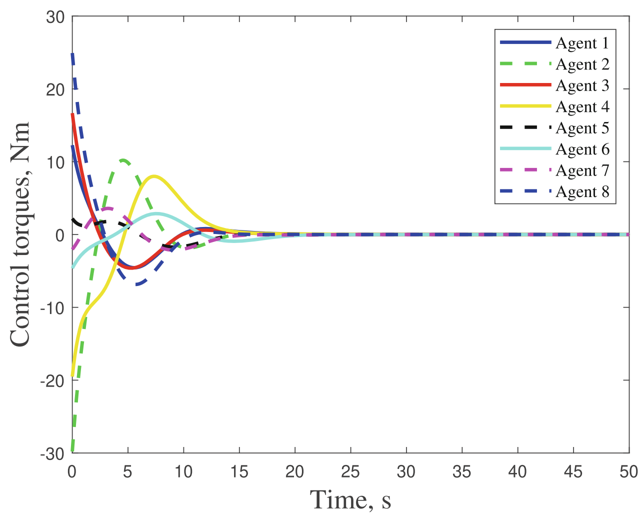

(C) The control torques $u_{i,3}$.

FIGURE 20 The control torques $\boldsymbol{u}_i = [u_{i,1}, u_{i,2}, u_{i,3}]^T$ in the example with IBR desired formation under the control law (41b).

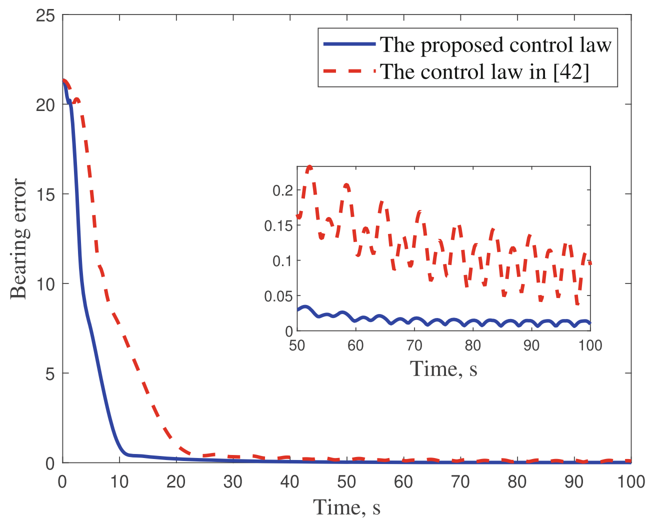

FIGURE 21 The equivalent bearing errors $\sum_{(i,j)\in\mathcal{E}} \|\boldsymbol{b}_{ij} - \boldsymbol{b}_{ij}^{\star}\|$ between the proposed bearing-based formation control law (41) and the bearing-based formation control law in Reference 42.

6 | CONCLUSION

In this article, the formation control problem for SMS is investigated by using the bearing measurement. Based on the BRT, two distributed bearing formation control laws are designed for SMS. In the first control law, each agent requires obtaining the global inertial frame. In the second control law, this requirement is removed, and each agent requires obtaining their local bearing and relative orientation measurements. Under the second control law, the inter-agent bearings converge to the desired bearing, and the orientation consensus of all agents is guaranteed. The system stability under the two control laws has been rigorously proved. Furthermore, the simulation results are given to verify the analysis.

FUNDING INFORMATION

This work was supported by the National Natural Science Foundation of China under Grant 61873312.

CONFLICT OF INTEREST STATEMENT

The authors have declared that no conflict of interest exists.

DATA AVAILABILITY STATEMENT

Data sharing not applicable to this article as no datasets were generated or analyzed during the current study.

ORCID

Chuang Xu https://orcid.org/0000-0001-8855-0522
Daniel Zelazo https://orcid.org/0000-0002-2931-245X

REFERENCES

1. Liu T, Jiang Z-P. Distributed formation control of nonholonomic mobile robots without global position measurements. *Automatica*. 2013;49(2):592-600.
2. Khoo S, Xie L, Man Z. Robust finite-time consensus tracking algorithm for multirobot systems. *IEEE/ASME Trans Mechatron*. 2009;14(2):219-228.
3. Wang W, Huang J, Wen C, Fan H. Distributed adaptive control for consensus tracking with application to formation control of nonholonomic mobile robots. *Automatica*. 2014;50(4):1254-1263.
4. He S, Xu Y, Wu Y, Li Y, Zhong W. Adaptive consensus tracking of multi-robotic systems via using integral sliding mode control. *Neurocomputing*. 2021;455:154-162.
5. Abdessameud A, Tayebi A. Formation control of vtol unmanned aerial vehicles with communication delays. *Automatica*. 2011;47(11):2383-2394.
6. Dong X, Yu B, Shi Z, Zhong Y. Time-varying formation control for unmanned aerial vehicles: Theories and applications. *IEEE Trans Control Syst Technol*. 2014;23(1):340-348.

7. Wei C, Luo J, Dai H, Duan G. Learning-based adaptive attitude control of spacecraft formation with guaranteed prescribed performance. *IEEE Trans Cybern*. 2018;49(11):4004-4016.
8. Zhao L, Yu J, Shi P. Command filtered backstepping-based attitude containment control for spacecraft formation. *IEEE Trans Syst Man Cybern Syst*. 2019;51(2):1278-1287.
9. Li X, Wen C, Chen C. Adaptive formation control of networked robotic systems with bearing-only measurements. *IEEE Trans Cybern*. 2020;51(1):199-209.
10. Oh K-K, Park M-C, Ahn H-S. A survey of multi-agent formation control. *Automatica*. 2015;53:424-440. https://www.sciencedirect.com/science/article/pii/S0005109814004038
11. He S, Lu Y, Wu Y, Li Y. Partial-information-based consensus of network systems with time-varying delay via sampled-data control. *Signal Process*. 2019;162:97-105.
12. Xiao F, Wang L, Chen J, Gao Y. Finite-time formation control for multi-agent systems. *Automatica*. 2009;45(11):2605-2611.
13. Lin Z, Wang L, Han Z, Fu M. A graph Laplacian approach to coordinate-free formation stabilization for directed networks. *IEEE Trans Autom Control*. 2015;61(5):1269-1280.
14. Wang C, Tnunay H, Zuo Z, Lennox B, Ding Z. Fixed-time formation control of multirobot systems: Design and experiments. *IEEE Trans Ind Electron*. 2018;66(8):6292-6301.
15. Oh K-K, Ahn H-S. Distance-based undirected formations of single-integrator and double-integrator modeled agents in n-dimensional space. *Int J Robust Nonlinear Control*. 2014;24(12):1809-1820.
16. Cai X, De Queiroz M. Adaptive rigidity-based formation control for multirobotic vehicles with dynamics. *IEEE Trans Control Syst Technol*. 2014;23(1):389-396.
17. Sun Z, Anderson BD, Deghat M, Ahn H-S. Rigid formation control of double-integrator systems. *Int J Control*. 2017;90(7):1403-1419.
18. Bishop AN, Shames I, Anderson BD. Stabilization of rigid formations with direction-only constraints. *2011 50th IEEE Conference on Decision and Control and European Control Conference*. IEEE; 2011:746-752.
19. Eren T. Formation shape control based on bearing rigidity. *Int J Control*. 2012;85(9):1361-1379.
20. Franchi A, Giordano PR. Decentralized control of parallel rigid formations with direction constraints and bearing measurements. *in 2012 IEEE 51st IEEE Conference on Decision and Control (CDC)*. IEEE; 2012:5310-5317.
21. Zelazo D, Franchi A, Giordano PR. Rigidity theory in se (2) for unscaled relative position estimation using only bearing measurements. *European Control Conference (ECC)*. Vol 2014. IEEE; 2014:2703-2708.
22. Zhao S, Zelazo D. Bearing rigidity and almost global bearing-only formation stabilization. *IEEE Trans Autom Control*. 2015;61(5):1255-1268.
23. Zhao S, Zelazo D. Localizability and distributed protocols for bearing-based network localization in arbitrary dimensions. *Automatica*. 2016;69:334-341.
24. Zhao S, Li Z, Ding Z. Bearing-only formation tracking control of multiagent systems. *IEEE Trans Autom Control*. 2019;64(11):4541-4554.
25. Montijano E, Cristofalo E, Zhou D, Schwager M, Saguees C. Vision-based distributed formation control without an external positioning system. *IEEE Trans Robot*. 2016;32(2):339-351.
26. Tian Y-P, Wang Q. Global stabilization of rigid formations in the plane. *Automatica*. 2013;49(5):1436-1441.
27. Trinh MH, Pham VH, Park M-C, Sun Z, Anderson BD, Ahn H-S. Comments on "Global stabilization of rigid formations in the plane". *Automatica*. 2017;77:393-396. [*Automatica*. 2013;49:1436-1441].
28. Mou S, Belabbas M-A, Morse AS, Sun Z, Anderson BD. Undirected rigid formations are problematic. *IEEE Trans Autom Control*. 2015;61(10):2821-2836.
29. Ahn H-S. *Formation Control*. Springer International Publishing; 2020. doi:10.1007/978-3-030-15187-4
30. Anderson BD, Yu C, Fidan B, Hendrickx JM. Rigid graph control architectures for autonomous formations. *IEEE Control Syst Mag*. 2008;28(6):48-63.
31. Zhao S, Zelazo D. Bearing rigidity theory and its applications for control and estimation of network systems: Life beyond distance rigidity. *IEEE Control Syst Mag*. 2019;39(2):66-83.
32. Tron R, Thomas J, Loianno G, Daniilidis K, Kumar V. A distributed optimization framework for localization and formation control: Applications to vision-based measurements. *IEEE Control Syst Mag*. 2016;36(4):22-44.
33. Mao G, Fidan B, Anderson BD. Wireless sensor network localization techniques. *Comput Netw*. 2007;51(10):2529-2553.
34. Li Z, Tnunay H, Zhao S, Meng W, Xie SQ, Ding Z. Bearing-only formation control with prespecified convergence time. *IEEE Trans Cybern*. 2020;52(1):620-629.
35. Michieletto G, Cenedese A. Formation control for fully actuated systems: a quaternion-based bearing rigidity approach. *2019 18th European Control Conference (ECC), Naples, Italy*. IEEE; 2019:107-112.
36. Trinh MH, Van Tran Q, Van Vu D, Nguyen PD, Ahn H-S. Robust tracking control of bearing-constrained leader–follower formation. *Automatica*. 2021;131:109733.
37. Cai H, Huang J. The leader-following attitude control of multiple rigid spacecraft systems. *Automatica*. 2014;50(4):1109-1115.
38. Polyakov A. Nonlinear feedback design for fixed-time stabilization of linear control systems. *IEEE Trans Autom Control*. 2012;57(8):2106-U1. https://ieeexplore.ieee.org/document/6104367/
39. Zuo Z, Tie L. Distributed robust finite-time nonlinear consensus protocols for multi-agent systems. *Int J Syst Sci*. 2016;47(6):1366-1375.
40. Ito T. A Filippo solution of a system of differential equations with discontinuous right-hand sides. *Econ Lett*. 1979;4(4):349-354.
41. Angeli D, Praly L. Stability robustness in the presence of exponentially unstable isolated equilibria. *IEEE Trans Autom Control*. 2010;56(7):1582-1592.

42. Zhao J, Yu X, Li X, Wang H. Bearing-only formation tracking control of multi-agent systems with local reference frames and constant-velocity leaders. *IEEE Control Syst Lett*. 2020;5(1):1-6.
43. Cortes J. Discontinuous dynamical systems. *IEEE Control Syst Mag*. 2008;28(3):36-73.
44. Krastanov M. Forward invariant sets, homogeneity and small-time local controllability," Nonlinear Control and Differential Inclusions (Banach Center Publ 32). *Polish Acad Sci Warsaw*. 1995;32(1):287-300.

How to cite this article: Xu C, Zelazo D, Wu B. Bearing-based formation control of second-order multiagent systems with bounded disturbances. *Int J Robust Nonlinear Control*. 2024;34(1):167-199. doi: 10.1002/rnc.6966

APPENDIX A. PROOF OF THEOREM 1

Proof. The Filippov solution is considered in this proof, since the controller (14) is not continuous. Consider the Lyapunov function

$$V_{sv} = \frac{1}{2}\sum_{i=1}^{n} \boldsymbol{s}_{vi}^T \boldsymbol{s}_{vi}. \tag{A1}$$

The dynamics for $\boldsymbol{s}_{vi}$ is

$$\begin{aligned}\dot{\boldsymbol{s}}_{vi} &= \dot{\boldsymbol{v}}_i - \dot{\boldsymbol{v}}_{vi}\\ &\in \mathcal{K}\left(-\alpha_1\boldsymbol{s}_{vi} - \alpha_2\text{sig}^{r_1}(\boldsymbol{s}_{vi}) - \alpha_3\text{sig}^{r_2}(\boldsymbol{s}_{vi}) - \alpha_4\text{sign}(\boldsymbol{s}_{vi}) + \boldsymbol{\Delta}_{mi} - \dot{\boldsymbol{v}}_{vi}\right)\\ &\in \mathcal{K}\left(-\alpha_1\boldsymbol{s}_{vi} - \alpha_2\text{sig}^{r_1}(\boldsymbol{s}_{vi}) - \alpha_3\text{sig}^{r_2}(\boldsymbol{s}_{vi}) + \boldsymbol{\Delta}_{mi} - \dot{\boldsymbol{v}}_{vi}\right) - \alpha_4\mathcal{K}\left(\text{sign}(\boldsymbol{s}_{vi})\right)\\ &\in -\alpha_1\boldsymbol{s}_{vi} - \alpha_2\text{sig}^{r_1}(\boldsymbol{s}_{vi}) - \alpha_3\text{sig}^{r_2}(\boldsymbol{s}_{vi}) + \boldsymbol{\Delta}_{mi} - \dot{\boldsymbol{v}}_{vi} - \alpha_4\mathcal{K}\left(\text{sign}(\boldsymbol{s}_{vi})\right),\end{aligned} \tag{A2}$$

where the following properties[43] are applied. (1) $\mathcal{K}(\mathbf{g}(\boldsymbol{x})) = \mathbf{g}(\boldsymbol{x})$ if $\mathbf{g}(\boldsymbol{x}) : \mathbb{R}^n \to \mathbb{R}^m$ is continuous at $\boldsymbol{x} \in \mathbb{R}^n$. (2) $\mathcal{K}(\mathbf{g}_1(\boldsymbol{x}) + \mathbf{g}_2(\boldsymbol{x})) \subseteq \mathcal{K}(\mathbf{g}_1(\boldsymbol{x})) + \mathcal{K}(\mathbf{g}_2(\boldsymbol{x}))$ if $\mathbf{g}_1(\boldsymbol{x}), \mathbf{g}_2(\boldsymbol{x}) : \mathbb{R}^n \to \mathbb{R}^m$ are locally bounded at $\boldsymbol{x} \in \mathbb{R}^n$.

Substituting (A2) into $\dot{V}_{sv}$ yields

$$\begin{aligned}\dot{V}_{sv} &= \sum_{i=1}^{n} \boldsymbol{s}_{vi}^T\dot{\boldsymbol{s}}_{vi}\\ &\in \sum_{i=1}^{n}\left(-\alpha_1\|\boldsymbol{s}_{vi}\|^2 - \alpha_2\|\boldsymbol{s}_{vi}\|^{1+r_1} - \alpha_3\|\boldsymbol{s}_{vi}\|^{1+r_2} + \boldsymbol{s}_{vi}^T\boldsymbol{\Delta}_{mi} - \boldsymbol{s}_{vi}^T\dot{\boldsymbol{v}}_{vi} - \alpha_4\mathcal{K}\left(\boldsymbol{s}_{vi}^T\text{sign}(\boldsymbol{s}_{vi})\right)\right),\end{aligned} \tag{A3}$$

where the property[43]: $\mathbf{g}_1(\boldsymbol{x})\mathcal{K}(\mathbf{g}_2(\boldsymbol{x})) = \mathcal{K}(\mathbf{g}_1(\boldsymbol{x})\mathbf{g}_2(\boldsymbol{x}))$ if $\mathbf{g}_1(\boldsymbol{x}) : \mathbb{R}^n \to \mathbb{R}^m$ is continuous at $\boldsymbol{x} \in \mathbb{R}^n$ and $\mathbf{g}_2(\boldsymbol{x}) : \mathbb{R}^n \to \mathbb{R}^m$ is locally bounded at $\boldsymbol{x} \in \mathbb{R}^n$, is applied.

Note that $\mathcal{K}\left(\boldsymbol{s}_{vi}^T\text{sign}(\boldsymbol{s}_{vi})\right) = \mathcal{K}(\|\boldsymbol{s}_{vi}\|_1) = \|\boldsymbol{s}_{vi}\|_1 \geq \|\boldsymbol{s}_{vi}\|$, where $\|\bullet\|_1$ denotes 1-norm. Then, (A3) becomes

$$\begin{aligned}\dot{V}_{sv} &\leq \sum_{i=1}^{n}\left(-\alpha_1\|\boldsymbol{s}_{vi}\|^2 - \alpha_2\|\boldsymbol{s}_{vi}\|^{1+r_1} - \alpha_3\|\boldsymbol{s}_{vi}\|^{1+r_2} - \alpha_4\|\boldsymbol{s}_{vi}\| + \boldsymbol{s}_{vi}^T\boldsymbol{\Delta}_{mi} - \boldsymbol{s}_{vi}^T\dot{\boldsymbol{v}}_{vi}\right)\\ &\leq -\sum_{i=1}^{n}\left(\alpha_1\|\boldsymbol{s}_{vi}\|^2 + \alpha_2\|\boldsymbol{s}_{vi}\|^{1+r_1} + \alpha_3\|\boldsymbol{s}_{vi}\|^{1+r_2} + (\alpha_4 - \epsilon_1 - \|\dot{\boldsymbol{v}}_{vi}\|)\|\boldsymbol{s}_{vi}\|\right).\end{aligned} \tag{A4}$$

The time derivative of $\boldsymbol{v}_{vi}$ is

$$\dot{\boldsymbol{v}}_{vi} = \alpha_5\sum_{j\in\mathcal{N}_i}\left(\dot{\boldsymbol{b}}_{ij}\boldsymbol{b}_{ij}^T + \boldsymbol{b}_{ij}\dot{\boldsymbol{b}}_{ij}^T\right)\boldsymbol{b}_{ij}^{\star}, \tag{A5}$$

with

$$\dot{\boldsymbol{b}}_{ij} = \frac{1}{\|\boldsymbol{x}_{ij}\|}\boldsymbol{P}(\boldsymbol{b}_{ij})(\boldsymbol{v}_j - \boldsymbol{v}_i). \tag{A6}$$

In this proof, the forward-invariant set theory[44] is used to analyze the stability. First, the following set is constructed.

$$\Gamma_1 = \{(\boldsymbol{v}_1, \dots, \boldsymbol{v}_n) \mid \|\boldsymbol{v}_i\| \leq V_{M1}, i = 1, \dots, n\}. \tag{A7}$$

In the set Γ_1, the velocities $\boldsymbol{v}_i$ are bounded by $\|\boldsymbol{v}_i\| \leq V_{M1}$. According to Assumption 2, the terms $\frac{1}{\|\boldsymbol{x}_{ij}\|}$ are bounded by $\frac{1}{\|\boldsymbol{x}_{ij}\|} \leq \frac{1}{d_{\min}}$. Then, in the set Γ_1, $\dot{\boldsymbol{b}}_{ij}$ is bounded by

$$\begin{aligned}
\|\dot{\boldsymbol{b}}_{ij}\| &\leq \frac{1}{\|\boldsymbol{x}_{ij}\|}\|\boldsymbol{P}(\boldsymbol{b}_{ij})\|\|(\boldsymbol{v}_j - \boldsymbol{v}_i)\| \\
&\leq \frac{1}{d_{\min}}\|\boldsymbol{P}(\boldsymbol{b}_{ij})\|(\|\boldsymbol{v}_j\| + \|\boldsymbol{v}_i\|) \\
&\leq \frac{2V_{M1}}{d_{\min}}
\end{aligned} \tag{A8}$$

where the property $\|\boldsymbol{P}(\boldsymbol{b}_{ij})\| = 1$ is applied.

In view of (A5) and (A8), in the set Γ_1, $\dot{\boldsymbol{v}}_{vi}$ is bounded by

$$\begin{aligned}
\|\dot{\boldsymbol{v}}_{vi}\| &\leq \alpha_5 \sum_{j\in\mathcal{N}_i}\left(\|\dot{\boldsymbol{b}}_{ij}\|\|\boldsymbol{b}_{ij}^T\| + \|\boldsymbol{b}_{ij}\|\|\dot{\boldsymbol{b}}_{ij}^T\|\right)\|\boldsymbol{b}_{ij}^{\star}\| \\
&= 2\alpha_5 \sum_{j\in\mathcal{N}_i}\|\dot{\boldsymbol{b}}_{ij}\| \leq \max_{i=1,\dots,n}\{|\mathcal{N}_i|\}\frac{4\alpha_5 V_{M1}}{d_{\min}}.
\end{aligned} \tag{A9}$$

Invoking Lemma 2, we have

$$\alpha_2 \sum_{i=1}^{n}\|\boldsymbol{s}_{vi}\|^{1+r_1} \geq \alpha_2\left\{\sum_{i=1}^{n}\boldsymbol{s}_{vi}^T\boldsymbol{s}_{vi}\right\}^{\frac{1+r_1}{2}}, \tag{A10}$$

and

$$\alpha_3 \sum_{i=1}^{n}\|\boldsymbol{s}_{vi}\|^{1+r_2} \geq \alpha_3 n^{\frac{1-r_2}{2}}\left\{\sum_{i=1}^{n}\boldsymbol{s}_{vi}^T\boldsymbol{s}_{vi}\right\}^{\frac{1+r_2}{2}}. \tag{A11}$$

Substituting (A9)–(A11) into (A4) gives

$$\begin{aligned}
\dot{V}_{sv} &\leq -\alpha_2 2^{\frac{1+r_1}{2}}\left\{\frac{1}{2}\sum_{i=1}^{n}\boldsymbol{s}_{vi}^T\boldsymbol{s}_{vi}\right\}^{\frac{1+r_1}{2}} - \alpha_3 2^{\frac{1+r_2}{2}} n^{\frac{1-r_2}{2}}\left\{\frac{1}{2}\sum_{i=1}^{n}\boldsymbol{s}_{vi}^T\boldsymbol{s}_{vi}\right\}^{\frac{1+r_2}{2}} \\
&= -\eta_1 V_{sv}^{\frac{1+r_1}{2}} - \eta_2 V_{sv}^{\frac{1+r_2}{2}},
\end{aligned} \tag{A12}$$

where $\eta_1 = \alpha_2 2^{\frac{1+r_1}{2}}$ and $\eta_2 = \alpha_3 2^{\frac{1+r_2}{2}} n^{\frac{1-r_2}{2}}$. According to Lemma 1, it follows from (A12) that the errors $\boldsymbol{s}_{vi}$ converges to the origin in the time T_1 in the set Γ_1.

Since the virtual velocities $\boldsymbol{v}_{vi}$ and the errors $\boldsymbol{s}_{vi}$ are bounded, it follows that $\boldsymbol{v}_i$ are bounded, which implies that the set Γ_1 is a forward-invariant set.[44] This means that $\boldsymbol{v}_i \in \Gamma_1$ always holds if $\boldsymbol{v}_i(0) \in \Gamma_1$. Thus, the errors $\boldsymbol{s}_{vi}$ converge to the origin in the time T_1 under the control law (14) if $\boldsymbol{v}_i(0) \in \Gamma_1$. ■

APPENDIX B. PROOF OF THEOREM 4

Proof. The Filippov solution is considered in this proof, since the controller (41) is not continuous. Consider the Lyapunov function

$$V_s = \frac{1}{2}\sum_{i=1}^{n}\left(\boldsymbol{s}_{vi}^b\right)^T\boldsymbol{s}_{vi}^b + \frac{1}{2}\sum_{i=1}^{n}\boldsymbol{s}_{\omega i}^T\boldsymbol{J}_i\boldsymbol{s}_{\omega i}. \tag{B1}$$

Substituting (41) into $\dot{V}_s$ yields

$$
\begin{aligned}
\dot{V}_s &= \sum_{i=1}^{n} (\boldsymbol{s}_{vi}^b)^T \left(\dot{\boldsymbol{v}}_i^b - \dot{\boldsymbol{v}}_{vi}^b\right) + \sum_{i=1}^{n} \boldsymbol{s}_{\omega i}^T \boldsymbol{J}_i (\dot{\boldsymbol{\omega}}_i - \dot{\boldsymbol{\omega}}_{vi}) \\
&\in -\sum_{i=1}^{n} \left(\beta_1 \|\boldsymbol{s}_{vi}^b\|^2 + \beta_2 \|\boldsymbol{s}_{vi}^b\|^{1+r_3} + \beta_3 \|\boldsymbol{s}_{vi}^b\|^{1+r_4} + \beta_4 \mathcal{K}\left((\boldsymbol{s}_{vi}^b)^T \mathrm{sign}\left(\boldsymbol{s}_{vi}^b\right)\right) - -(\boldsymbol{s}_{vi}^b)^T (\dot{\boldsymbol{v}}_{vi}^b + \boldsymbol{\Delta}_{mi})\right) \\
&\quad - \sum_{i=1}^{n} \left(\gamma_1 \|\boldsymbol{s}_{\omega i}\|^2 + \gamma_2 \|\boldsymbol{s}_{\omega i}\|^{1+r_3} + \gamma_3 \|\boldsymbol{s}_{\omega i}\|^{1+r_4} + \gamma_4 \mathcal{K}\left(\boldsymbol{s}_{\omega i}^T \mathrm{sign}\left(\boldsymbol{s}_{\omega i}\right)\right) - \boldsymbol{s}_{\omega i}^T (\dot{\boldsymbol{\omega}}_{vi} + \boldsymbol{\Delta}_{ai})\right),
\end{aligned} \tag{B2}
$$

where the following properties[43] are applied. (1) $\mathcal{K}(\boldsymbol{g}(\boldsymbol{x})) = \boldsymbol{g}(\boldsymbol{x})$ if $\boldsymbol{g}(\boldsymbol{x}) : \mathbb{R}^n \to \mathbb{R}^m$ is continuous at $\boldsymbol{x} \in \mathbb{R}^n$. (2) $\mathcal{K}(\boldsymbol{g}_1(\boldsymbol{x}) + \boldsymbol{g}_2(\boldsymbol{x})) \subseteq \mathcal{K}(\boldsymbol{g}_1(\boldsymbol{x})) + \mathcal{K}(\boldsymbol{g}_2(\boldsymbol{x}))$ if $\boldsymbol{g}_1(\boldsymbol{x}), \boldsymbol{g}_2(\boldsymbol{x}) : \mathbb{R}^n \to \mathbb{R}^m$ are locally bounded at $\boldsymbol{x} \in \mathbb{R}^n$. (3) $\boldsymbol{g}_1(\boldsymbol{x})\mathcal{K}(\boldsymbol{g}_2(\boldsymbol{x})) = \mathcal{K}(\boldsymbol{g}_1(\boldsymbol{x})\boldsymbol{g}_2(\boldsymbol{x}))$ if $\boldsymbol{g}_1(\boldsymbol{x}) : \mathbb{R}^n \to \mathbb{R}^m$ is continuous at $\boldsymbol{x} \in \mathbb{R}^n$ and $\boldsymbol{g}_2(\boldsymbol{x}) : \mathbb{R}^n \to \mathbb{R}^m$ is locally bounded at $\boldsymbol{x} \in \mathbb{R}^n$.

Note that $\mathcal{K}\left((\boldsymbol{s}_{vi}^b)^T \mathrm{sign}\left(\boldsymbol{s}_{vi}^b\right)\right) = \mathcal{K}\left(\|\boldsymbol{s}_{vi}^b\|_1\right) = \|\boldsymbol{s}_{vi}^b\|_1 \geq \|\boldsymbol{s}_{vi}^b\|$ and $\mathcal{K}\left(\boldsymbol{s}_{\omega i}^T \mathrm{sign}(\boldsymbol{s}_{\omega i})\right) = \mathcal{K}(\|\boldsymbol{s}_{\omega i}\|_1) = \|\boldsymbol{s}_{\omega i}\|_1 \geq \|\boldsymbol{s}_{\omega i}\|$. Then, (B2) becomes

$$
\begin{aligned}
\dot{V}_s &\in -\sum_{i=1}^{n} \left(\beta_1 \|\boldsymbol{s}_{vi}^b\|^2 + \beta_2 \|\boldsymbol{s}_{vi}^b\|^{1+r_3} + \beta_3 \|\boldsymbol{s}_{vi}^b\|^{1+r_4} + \beta_4 \|\boldsymbol{s}_{vi}^b\| - \left(\boldsymbol{s}_{vi}^b\right)^T \left(\dot{\boldsymbol{v}}_{vi}^b + \boldsymbol{\Delta}_{mi}\right)\right) \\
&\quad - \sum_{i=1}^{n} \left(\gamma_1 \|\boldsymbol{s}_{\omega i}\|^2 + \gamma_2 \|\boldsymbol{s}_{\omega i}\|^{1+r_3} + \gamma_3 \|\boldsymbol{s}_{\omega i}\|^{1+r_4} + \gamma_4 \|\boldsymbol{s}_{\omega i}\| - \boldsymbol{s}_{\omega i}^T (\dot{\boldsymbol{\omega}}_{vi} + \boldsymbol{\Delta}_{ai})\right) \\
&\leq -\sum_{i=1}^{n} \left(\beta_1 \|\boldsymbol{s}_{vi}^b\|^2 + \beta_2 \|\boldsymbol{s}_{vi}^b\|^{1+r_3} + \beta_3 \|\boldsymbol{s}_{vi}^b\|^{1+r_4}\right) \\
&\quad - \sum_{i=1}^{n} \left(\beta_4 - \epsilon_1 - \|\boldsymbol{R}(\boldsymbol{Q}_i)\boldsymbol{\omega}_i^{\times} \boldsymbol{R}^T(\boldsymbol{Q}_i)\boldsymbol{v}_i^b\| - \|\dot{\boldsymbol{v}}_{vi}^b\|\right) \|\boldsymbol{s}_{vi}\| \\
&\quad - \sum_{i=1}^{n} \left(\gamma_1 \|\boldsymbol{s}_{\omega i}\|^2 + \gamma_2 \|\boldsymbol{s}_{\omega i}\|^{1+r_3} + \gamma_3 \|\boldsymbol{s}_{\omega i}\|^{1+r_4} + (\gamma_4 - \epsilon_2 - \|\dot{\boldsymbol{\omega}}_{vi}\|)\|\boldsymbol{s}_{\omega i}\|\right).
\end{aligned} \tag{B3}
$$

The time derivatives of $\boldsymbol{v}_{vi}$ and $\boldsymbol{\omega}_{vi}$ are respectively

$$
\begin{aligned}
\dot{\boldsymbol{v}}_{vi}^b &= \beta_5 \sum_{j \in \mathcal{N}_i} \left(\dot{\boldsymbol{b}}_{ij}^b \left(\boldsymbol{b}_{ij}^b\right)^T + \boldsymbol{b}_{ij}^b \left(\dot{\boldsymbol{b}}_{ij}^b\right)^T\right) \left(\boldsymbol{I}_3 + \boldsymbol{R}(\boldsymbol{Q}_{ij})\right) \boldsymbol{b}_{ij}^{b\star} \\
&\quad - \beta_5 \sum_{j \in \mathcal{N}_i} \boldsymbol{P}\left(\boldsymbol{b}_{ij}^b\right) \boldsymbol{R}(\boldsymbol{Q}_{ij}) \boldsymbol{\omega}_{ij}^{\times} \boldsymbol{b}_{ij}^{b\star} + \beta_5 \sum_{j \in \mathcal{N}_i} \boldsymbol{P}\left(\boldsymbol{b}_{ij}^b\right) \left(\boldsymbol{I}_3 + \boldsymbol{R}(\boldsymbol{Q}_{ij})\right) \boldsymbol{\omega}_i^{\times} \boldsymbol{b}_{ij}^{b\star},
\end{aligned} \tag{B4}
$$

and

$$
\begin{aligned}
\dot{\boldsymbol{\omega}}_{vi} &= -\gamma_5 \sum_{j \in \mathcal{N}_i} \left(\boldsymbol{E}^T(\dot{\boldsymbol{Q}}_{ij})\boldsymbol{q}_{ij} + \boldsymbol{E}^T(\boldsymbol{Q}_{ij})\boldsymbol{E}(\boldsymbol{Q}_{ij})\boldsymbol{\omega}_{ij} - \boldsymbol{R}(\boldsymbol{Q}_{ij})\boldsymbol{\omega}_{ij}^{\times} \boldsymbol{E}^T(\boldsymbol{Q}_{ji})\boldsymbol{q}_{ji}\right. \\
&\quad \left. - \boldsymbol{R}(\boldsymbol{Q}_{ij})\boldsymbol{E}^T(\dot{\boldsymbol{Q}}_{ji})\boldsymbol{q}_{ji} - \boldsymbol{R}(\boldsymbol{Q}_{ij})\boldsymbol{E}^T(\boldsymbol{Q}_{ji})\boldsymbol{E}(\boldsymbol{Q}_{ij})\boldsymbol{\omega}_{ij}\right),
\end{aligned} \tag{B5}
$$

where

$$
\begin{cases}
\dot{\boldsymbol{b}}_{ij}^b = \{\boldsymbol{b}_{ij}^b\}^{\times} \boldsymbol{\omega}_i + \frac{1}{\|\boldsymbol{x}_{ij}\|} \boldsymbol{P}\left(\boldsymbol{b}_{ij}^b\right) \left[\boldsymbol{R}^T(\boldsymbol{Q}_i)\boldsymbol{R}\left(\boldsymbol{Q}_j\right)\boldsymbol{v}_j^b - \boldsymbol{v}_i^b\right] \\
\dot{\boldsymbol{Q}}_{ij} = \frac{1}{2} \boldsymbol{M}\left(\boldsymbol{Q}_{ij}\right) \boldsymbol{\omega}_{ij}^{+} \\
\boldsymbol{\omega}_{ij} = \boldsymbol{\omega}_i - \boldsymbol{R}(\boldsymbol{Q}_{ij})\boldsymbol{\omega}_j
\end{cases}. \tag{B6}
$$

In this proof, the forward-invariant set theory[44] is used to analyze the stability. First, consider the set

$$
\Gamma_2 = \left\{\left\{\left(\boldsymbol{v}_1^b, \boldsymbol{\omega}_i\right), \ldots, \left(\boldsymbol{v}_n^b, \boldsymbol{\omega}_n\right)\right\} \mid \|\boldsymbol{v}_i^b\| \leq V_{M2}, \|\boldsymbol{\omega}_i\| \leq V_{M3}, i = 1, \ldots, n\right\}. \tag{B7}
$$

In the set Γ_2, $\boldsymbol{v}_i^b$ and $\boldsymbol{\omega}_i$ are bounded by $\|\boldsymbol{v}_i^b\| \leq V_{M2}$ and $\|\boldsymbol{\omega}_i\| \leq V_{M3}$, respectively. According to Assumption 2, the terms $\frac{1}{\|\boldsymbol{x}_{ij}\|}$ are bounded by $\frac{1}{\|\boldsymbol{x}_{ij}\|} \leq \frac{1}{d_{\min}}$. Then, it follows from (B4) and (B6) that in the set Γ_2, $\dot{\boldsymbol{v}}_{vi}^b$ is bounded by

$$\begin{aligned} \|\dot{\boldsymbol{v}}_{vi}^b\| &\leq 2\beta_5 \sum_{j\in\mathcal{N}_i} \|\dot{\boldsymbol{b}}_{ij}^b\| \|\boldsymbol{b}_{ij}^b\| \|\boldsymbol{I}_3 + \boldsymbol{R}(\boldsymbol{Q}_{ij})\| \|\boldsymbol{b}_{ij}^{b\star}\| + \beta_5 \sum_{j\in\mathcal{N}_i} \|\boldsymbol{P}(\boldsymbol{b}_{ij}^b)\| \|\boldsymbol{R}(\boldsymbol{Q}_{ij})\| \|\boldsymbol{\omega}_{ij}^\times\| \|\boldsymbol{b}_{ij}^{b\star}\| \\ &\quad + \beta_5 \sum_{j\in\mathcal{N}_i} \|\boldsymbol{P}(\boldsymbol{b}_{ij}^b)\| \|\boldsymbol{I}_3 + \boldsymbol{R}(\boldsymbol{Q}_{ij})\| \|\boldsymbol{\omega}_i^\times\| \|\boldsymbol{b}_{ij}^{b\star}\| \\ &\leq \beta_5 \sum_{j\in\mathcal{N}_i} \left(4\|\dot{\boldsymbol{b}}_{ij}^b\| + V_{M2} + 3V_{M3}\right) \\ &\leq \beta_5 \max_{i=1,\dots,n}\{|\mathcal{N}_i|\} \left(\frac{8V_{M2}}{d_{\min}} + V_{M2} + 7V_{M3}\right), \end{aligned} \tag{B8}$$

where the property $\|\boldsymbol{R}(\boldsymbol{Q}_{ij})\| = 1$ is applied in (B8).

In the set Γ_2, one has

$$\|\boldsymbol{R}(\boldsymbol{Q}_i)\boldsymbol{\omega}_i^\times \boldsymbol{R}^T(\boldsymbol{Q}_i)\boldsymbol{v}_i^b\| \leq \|\boldsymbol{\omega}_i\| \|\boldsymbol{v}_i^b\| \leq V_{M2}V_{M3} \tag{B9}$$

Note that

$$\begin{aligned} \|\boldsymbol{E}(\dot{\boldsymbol{Q}}_{ij})\| &= \|\dot{q}_{0,ij}\boldsymbol{I}_3 + \dot{\boldsymbol{q}}_{ij}^\times\| \\ &\leq \|\dot{q}_{0,ij}\boldsymbol{I}_3\| + \|\dot{\boldsymbol{q}}_{ij}^\times\| \\ &= \left\|\frac{1}{2}\boldsymbol{q}_{ij}^T\boldsymbol{\omega}_{ij}\right\| + \left\|\left(\frac{1}{2}\boldsymbol{E}(\boldsymbol{Q}_{ij})\boldsymbol{\omega}_{ij}\right)^\times\right\| \\ &\leq 2V_{M3}. \end{aligned} \tag{B10}$$

It follows from (B5), (B6) and (B10) that in the set Γ_2, $\dot{\boldsymbol{\omega}}_{vi}$ is bounded by

$$\begin{aligned} \|\dot{\boldsymbol{\omega}}_{vi}\| &\leq \gamma_5 \sum_{j\in\mathcal{N}_i} \Big(\|\boldsymbol{E}(\dot{\boldsymbol{Q}}_{ij})\| \|\boldsymbol{q}_{ij}\| + \|\boldsymbol{E}(\boldsymbol{Q}_{ij})\|^2 \|\boldsymbol{\omega}_{ij}\| + \|\boldsymbol{R}(\boldsymbol{Q}_{ij})\| \|\boldsymbol{\omega}_{ij}^\times\| \|\boldsymbol{E}(\boldsymbol{Q}_{ji})\| \|\boldsymbol{q}_{ji}\| \\ &\quad + \|\boldsymbol{R}(\boldsymbol{Q}_{ij})\| \|\boldsymbol{E}(\dot{\boldsymbol{Q}}_{ji})\| \|\boldsymbol{q}_{ji}\| + \|\boldsymbol{R}(\boldsymbol{Q}_{ij})\| \|\boldsymbol{E}(\boldsymbol{Q}_{ji})\| \|\boldsymbol{E}(\boldsymbol{Q}_{ij})\| \|\boldsymbol{\omega}_{ij}\| \Big) \\ &\leq 10\gamma_5 V_{M3} \max_{i=1,\dots,n}\{|\mathcal{N}_i|\} \leq \gamma_4 - \epsilon_2, \end{aligned} \tag{B11}$$

where the properties $\|\boldsymbol{R}(\boldsymbol{Q}_{ij})\| = \|\boldsymbol{R}(\boldsymbol{Q}_{ji})\| = 1$, $\|\boldsymbol{E}(\boldsymbol{Q}_{ij})\| \leq 1$ and $\|\boldsymbol{q}_{ij}\| = \|\boldsymbol{q}_{ji}\| \leq 1$ are applied in (B11).

Invoking Lemma 2, we have

$$k_{f2}^b \sum_{i=1}^n \|\boldsymbol{s}_{vi}^b\|^{1+r_3} \geq k_{f2}^b \left\{ \sum_{i=1}^n \|\boldsymbol{s}_{vi}^b\|^2 \right\}^{\frac{1+r_3}{2}}, \tag{B12}$$

$$k_{f3}^b \sum_{i=1}^n \|\boldsymbol{s}_{vi}^b\|^{1+r_4} \geq k_{f3}^b n^{\frac{1-r_4}{2}} \left\{ \sum_{i=1}^n \|\boldsymbol{s}_{vi}^b\|^2 \right\}^{\frac{1+r_4}{2}}, \tag{B13}$$

$$\gamma_2 \sum_{i=1}^n \|\boldsymbol{s}_{\omega i}\|^{1+r_3} \geq \gamma_2 \left\{ \sum_{i=1}^n \|\boldsymbol{s}_{\omega i}\|^2 \right\}^{\frac{1+r_3}{2}} \geq \gamma_2 \left\{ \frac{1}{\lambda_{\max}(\boldsymbol{J})} \sum_{i=1}^n \boldsymbol{s}_{\omega i}^T \boldsymbol{J}_i \boldsymbol{s}_{\omega i} \right\}^{\frac{1+r_3}{2}}, \tag{B14}$$

and

$$\gamma_3 \sum_{i=1}^n \|\boldsymbol{s}_{\omega i}\|^{1+r_4} \geq \gamma_3 n^{\frac{1-r_4}{2}} \left\{ \sum_{i=1}^n \|\boldsymbol{s}_{\omega i}\|^2 \right\}^{\frac{1+r_4}{2}} \geq \gamma_3 n^{\frac{1-r_4}{2}} \left\{ \frac{1}{\lambda_{\max}(\boldsymbol{J})} \sum_{i=1}^n \boldsymbol{s}_{\omega i}^T \boldsymbol{J}_i \boldsymbol{s}_{\omega i} \right\}^{\frac{1+r_4}{2}}. \tag{B15}$$

Substituting (B8), (B9) and (B11)–(B15) into (B3) yields

$$\begin{aligned}
\dot{V}_s \leq & -\beta_2\left\{\sum_{i=1}^{n}\|\boldsymbol{s}_{vi}^b\|^2\right\}^{\frac{1+r_3}{2}} - \beta_3 n^{\frac{1-r_4}{2}}\left\{\sum_{i=1}^{n}\|\boldsymbol{s}_{vi}^b\|^2\right\}^{\frac{1+r_4}{2}} \\
& - \gamma_2\left\{\frac{1}{\lambda_{\max}(\boldsymbol{J})}\sum_{i=1}^{n}\boldsymbol{s}_{\omega i}^T\boldsymbol{J}_i\boldsymbol{s}_{\omega i}\right\}^{\frac{1+r_3}{2}} - \gamma_3 n^{\frac{1-r_4}{2}}\left\{\frac{1}{\lambda_{\max}(\boldsymbol{J})}\sum_{i=1}^{n}\boldsymbol{s}_{\omega i}^T\boldsymbol{J}_i\boldsymbol{s}_{\omega i}\right\}^{\frac{1+r_4}{2}} \\
\leq & -\min\left\{\beta_2, \frac{\gamma_2}{\lambda_{\max}^{\frac{1+r_3}{2}}(\boldsymbol{J})}\right\}\left\{\sum_{i=1}^{n}\left(\boldsymbol{s}_{vi}^b\right)^T\boldsymbol{s}_{vi}^b + \sum_{i=1}^{n}\boldsymbol{s}_{\omega i}^T\boldsymbol{J}_i\boldsymbol{s}_{\omega i}\right\}^{\frac{1+r_3}{2}} \\
& - (2n)^{\frac{1-r_4}{2}}\min\left\{\beta_3, \frac{\gamma_3}{\lambda_{\max}^{\frac{1+r_4}{2}}(\boldsymbol{J})}\right\}\left\{\sum_{i=1}^{n}\left(\boldsymbol{s}_{vi}^b\right)^T\boldsymbol{s}_{vi}^b + \sum_{i=1}^{n}\boldsymbol{s}_{\omega i}^T\boldsymbol{J}_i\boldsymbol{s}_{\omega i}\right\}^{\frac{1+r_4}{2}} \\
\leq & -\eta_3 V_s^{\frac{1+r_3}{2}} - \eta_4 V_s^{\frac{1+r_4}{2}},
\end{aligned} \tag{B16}$$

where Lemma 2 is applied to derive the second inequality, and

$$\begin{aligned}
\lambda_{\max}(\boldsymbol{J}) &= \max\{\lambda_{\max}(\boldsymbol{J}_1), \ldots, \lambda_{\max}(\boldsymbol{J}_n)\}\} \\
\eta_3 &= 2^{\frac{1+r_3}{2}}\min\left\{\beta_2, \frac{\gamma_2}{\lambda_{\max}^{\frac{1+r_3}{2}}(\boldsymbol{J})}\right\} \\
\eta_4 &= 2n^{\frac{1-r_4}{2}}\min\left\{\alpha_3, \frac{\gamma_3}{\lambda_{\max}^{\frac{1+r_4}{2}}(\boldsymbol{J})}\right\}.
\end{aligned} \tag{B17}$$

According to Lemma 1, it follows from (B16) that the errors $\boldsymbol{s}_{vi}^b$ and $\boldsymbol{s}_{\omega i}$ converge to the origin in the time T_2 in the set Γ_2.

Since $\boldsymbol{v}_{vi}^b$, $\boldsymbol{s}_{vi}^b$, $\boldsymbol{\omega}_{vi}$, and $\boldsymbol{s}_{\omega i}$ are bounded, one has that $\boldsymbol{v}_i^b$ and $\boldsymbol{\omega}_i$ are both bounded, which yields that the set Γ_2 is a forward-invariant set. This means that $\left(\boldsymbol{v}_i^b, \boldsymbol{\omega}_i\right) \in \Gamma_2$ always holds if $\left(\boldsymbol{v}_i^b(0), \boldsymbol{\omega}_i(0)\right) \in \Gamma_2$. Thus, the errors and $\boldsymbol{s}_{vi}^b$ and $\boldsymbol{s}_{\omega i}$ converge to the origin in T_2 under the control law in (41) if $\|\boldsymbol{v}_i^b(0)\| \leq V_{M2}$ and $\|\boldsymbol{\omega}_i(0)\| \leq V_{M3}$. ■

APPENDIX C. PROOF OF THEOREM 5

Proof. Consider the Lyapunov function

$$V_q = \frac{1}{2}\sum_{i=1}^{n}\sum_{j\in\mathcal{N}_i}\boldsymbol{q}_{ij}^T\boldsymbol{q}_{ij}. \tag{C1}$$

Then, the time derivative $\dot{V}_q$ is

$$\begin{aligned}
\dot{V}_q &= \sum_{i=1}^{n}\sum_{j\in\mathcal{N}_i}\boldsymbol{q}_{ij}^T\dot{\boldsymbol{q}}_{ij} \\
&= \frac{1}{2}\sum_{i=1}^{n}\sum_{j\in\mathcal{N}_i}\boldsymbol{q}_{ij}^T\boldsymbol{E}(\boldsymbol{Q}_{ij})(\boldsymbol{\omega}_i - \boldsymbol{R}(\boldsymbol{Q}_{ij})\boldsymbol{\omega}_j) \\
&= \frac{1}{2}\sum_{i=1}^{n}\sum_{j\in\mathcal{N}_i}\boldsymbol{q}_{ij}^T\boldsymbol{E}(\boldsymbol{Q}_{ij})\boldsymbol{R}(\boldsymbol{Q}_i)[\boldsymbol{R}^T(\boldsymbol{Q}_i)\boldsymbol{\omega}_i - \boldsymbol{R}^T(\boldsymbol{Q}_j)\boldsymbol{\omega}_j] \\
&= \frac{1}{2}\boldsymbol{q}_{\mathcal{G}}^T\mathrm{diag}\{\boldsymbol{E}(\boldsymbol{Q}_{ij})\boldsymbol{R}(\boldsymbol{Q}_i)\}\overline{\boldsymbol{H}}\mathrm{diag}\{\boldsymbol{R}^T(\boldsymbol{Q}_i)\}\boldsymbol{\omega}
\end{aligned} \tag{C2}$$

where $\boldsymbol{q}_{\mathcal{G}}^T = [\ \dots\ , \boldsymbol{q}_{ij}^T, \ \dots\ ]^T \in \mathbb{R}^{3m}$ for $(i,j) \in \mathcal{E}$, $\boldsymbol{\omega} = [\boldsymbol{\omega}_1^T, \ \dots\ , \boldsymbol{\omega}_n^T]^T$, and $\overline{\boldsymbol{H}} = \boldsymbol{H} \otimes \boldsymbol{I}_3$.

Invoking (41b), one has

$$\boldsymbol{R}^T(\boldsymbol{Q}_i)\boldsymbol{\omega}_{vi} = \gamma_5 \sum_{j\in\mathcal{N}_i} \left[\boldsymbol{R}^T(\boldsymbol{Q}_i)\boldsymbol{E}^T(\boldsymbol{Q}_{ij})\boldsymbol{q}_{ij} - \boldsymbol{R}^T(\boldsymbol{Q}_j)\boldsymbol{E}^T(\boldsymbol{Q}_{ji})\boldsymbol{q}_{ji}\right]. \tag{C3}$$

Define $\boldsymbol{\omega}_s = [\boldsymbol{\omega}_{s1}^T, \ \dots\ , \boldsymbol{\omega}_{sn}^T]^T$. Then, it follows from (C3) that

$$\mathrm{diag}\{\boldsymbol{R}^T(\boldsymbol{Q}_i)\}\boldsymbol{\omega}_s = -\gamma_5 \overline{\boldsymbol{H}}^T \mathrm{diag}\{\boldsymbol{R}^T(\boldsymbol{Q}_i)\boldsymbol{E}^T(\boldsymbol{Q}_{ij})\}\boldsymbol{q}_{\mathcal{G}}. \tag{C4}$$

According to Theorem 4, $\boldsymbol{\omega}_i = \boldsymbol{\omega}_{vi}$ after the time T_2. After the time T_2, we can replace $\boldsymbol{\omega}$ by $\boldsymbol{\omega}_s$. Then, substituting (C4) into (C2) yields

$$\begin{aligned}
\dot{V}_q &= \frac{1}{2}\boldsymbol{q}_{\mathcal{G}}^T \mathrm{diag}\{\boldsymbol{E}(\boldsymbol{Q}_{ij})\boldsymbol{R}(\boldsymbol{Q}_i)\}\overline{\boldsymbol{H}}\mathrm{diag}\{\boldsymbol{R}^T(\boldsymbol{Q}_i)\}\boldsymbol{\omega}_s \\
&= -\frac{1}{2}\gamma_5 \boldsymbol{q}_{\mathcal{G}}^T \underbrace{\mathrm{diag}\{\boldsymbol{E}(\boldsymbol{Q}_{ij})\boldsymbol{R}(\boldsymbol{Q}_i)\}\overline{\boldsymbol{H}}}_{\zeta}\underbrace{\overline{\boldsymbol{H}}^T \mathrm{diag}\{\boldsymbol{R}^T(\boldsymbol{Q}_i)\boldsymbol{E}^T(\boldsymbol{Q}_{ij})\}}_{\zeta^T}\boldsymbol{q}_{\mathcal{G}} \\
&= -\frac{1}{2}\gamma_5 \|\boldsymbol{\zeta}^T \boldsymbol{q}_{\mathcal{G}}\|^2 \\
&\leq -\gamma_5 \|\boldsymbol{\zeta}\|^2 V_q.
\end{aligned} \tag{C5}$$

Therefore, it is obtained from (C5) that $\lim_{t\to\infty} \boldsymbol{q}_{ij} = 0$. ∎